Supplementary Material (ESI) for Chemical Communications

Electronic Supporting Information

Water Soluble Luminescent Platinum Terpyridine Complexes with Glycosylated Acetylide and Arylacetylide Ligands. Photoluminescent Properties and Cytotoxicities

Dik-Lung Ma,[a] Tina Yuen-Ting Shum,[a] Fuyi Zhang,[a] Chi-Ming Che*[a] and Mengsu Yang[b]

[a] *Department of Chemistry and Open Laboratory of Chemical Biology of the Institute of Molecular Technology for Drug Discovery and Synthesis, The University of Hong Kong, Pokfulam Road, Hong Kong. E-mail: cmche@hku.hk*
[b] *Department of Biology and Chemistry, City University of Hong Kong, 83 Tat Chee Avenue, Kowloon, Hong Kong*

Experimental section

Materials. Human serum albumin (HSA), calf thymus DNA (ct DNA) were purchased from Sigma Chemical Co. Ltd. and purified by the literature method.[1] The DNA concentration per base pair and protein concentation were determined by UV/Vis absorption spectroscopy using the following molar extinction coefficients at the indicated wavelengths: calf thymus DNA, ε_{260} = 13200 bp cm^{-1} M^{-1};[2] HSA, ε_{279} = 35300 cm^{-1} M^{-1}. A plasmid DNA, pDR2 (10.7 kb), was purchased from Clontech Laboratories Inc. (Palo Alto, USA). Unless otherwise stated, DNA binding experiments were performed in aerated Tris buffer solutions (5 mM Tris, 50 mM NaCl, pH 7.2) at 20 °C. K_2PtCl_4 and $^tBu_3$terpy (4,4′,4″-tri-*tert*-butyl-2,2′:6′,2″-terpyridine) were obtained from Aldrich. Pentaacetated β-D-glucopyranose, β-D-galactopyranose and heptaacetated β-D-lactose, β-D-maltose were prepared using the established methods.[3] 2′,3′,4′,6′,2,3,6-hepta-*O*-acetyl-α-bromo-D-maltopyranose was prepared using the established Fischer protocol.[4] Reagents and solvents were reagent grade. Solvent evaporation was performed under reduced pressure below 40 ºC using rotary evaporation and some residues were followed by evacuation to constant sample weight. [Pt(terpy)Cl](CF_3SO_3) (**9**) and [Pt($^tBu_3$terpy)Cl](CF_3SO_3) were prepared by literature method.[5] The stock solutions (10 mM) of Pt^{II} complexes for titration studies were prepared in either DMSO or MeCN, and further dilution to designated concentrations was made using deionised water. All the stock solutions were kept at –20 °C in the dark between experiments.

HepG2 (hepatocellular cancer),[6] HeLa (human cervix epitheloid carcinoma), NCI-H460 (lung cancer), MCF-7 (breast cancer) and 293 (normal kidney) cells were obtained from American Type Culture Collection. SF-268 (brain cancer) was obtained from National Cancer Institute of NIH, USA. Cell proliferation Kit I (MTT) from Roche was used for cytotoxicity evaluation.

Physical measurement. Absorption spectra were recorded on a Perkin-Elmer Lambda 19 UV/Visible spectrophotometer. Emission spectra were recorded on a SPEX Fluorolog-2 Model fluorescence spectrophotometer. Emission lifetime measurements were performed with a Quanta Ray DCR-3 pulsed Nd:YAG laser system (pulse output 355 nm, 8 ns). Error limits were estimated: λ (±1 nm); τ (±10%); ϕ (±10%). ^{1}H and ^{13}C NMR spectra were recorded on a Bruker DPX-300 NMR spectrometer. Positive-ion mass spectra were recorded on a Finnigan MAT95 mass spectrometer. Elemental analysis was performed by the Institute of Chemistry at the Chinese Academy of Sciences, Beijing. Infrared spectra were recorded as Nujol mulls on a Bio-Rad FT-IR spectrometer. Flow

cytometry measurements were performed with an EPICS XL cytometer (Coulter Corporation, Miami, FL) equipped with an argon laser.

Spectroscopic titration. Solutions of the platinum(II) complexes (50 μM) were prepared in Tris buffer solutions (5 mM Tris, 50 mM NaCl, pH 7.2). Aliquots of a millimolar stock ct DNA solution (0–500 μM) were added. Absorption spectra were recorded in the 200–600 nm range, after equilibration at 20.0 °C for 10 min. Emission spectra were recorded in the 400–800 nm range, after equilibration at 20.0 °C for 10 min. The intrinsic binding constant, K, was determined from a plot of $D/\Delta\varepsilon_{ap}$ vs D according to equation (1):[7]

$$D/\Delta\varepsilon_{ap} = D/\Delta\varepsilon + 1/(\Delta\varepsilon \times K) \quad (1)$$

where D is the concentration of DNA, $\Delta\varepsilon_{ap} = |\varepsilon_A - \varepsilon_F|$, $\varepsilon_A = A_{obs}/[\text{complex}]$, and $\Delta\varepsilon = |\varepsilon_B - \varepsilon_F|$; ε_B and ε_F correspond to the extinction coefficients of DNA–complex adduct and unbound complex, respectively.

Restriction endonuclease fragmentation assay. Digestion of a plasmid pDR2 DNA (10.7 kb) with a restriction enzyme, ApaI (Boehringer Mannheim), was performed by mixing the DNA (21 nM bp^{-1}) in 1× SuRE/Cut Buffer A with ApaI (1 unit/μL), followed by incubation at 37 °C for 1 h.[7] A mixture of ethidium bromide (4 μM), Hoechst 33342 (200 μM), cisplatin (*cis*-$[Pt(NH_3)_2Cl_2]$) (200 μM), **1** (4 μM) and pDR2 (10.7 kbp, 21 nM bp^{-1}) in digestion buffer was first incubated at room temperature for 5 min followed by addition of restriction enzyme (1 unit/μL). Two controls of pDR2 in the absence and presence of restriction enzyme in digestion buffer were prepared. All the solutions were incubated at 37 °C for 1 h; after restriction enzyme digestion the samples were analysed by agarose gel electrophoresis.

Gel mobility shift assay. A 100-bp PCR product (15.2 μM bp^{-1}) was mixed with the metal complex at various DNA:complex ratios (1:10, 1:5 and 1:2.5). The mixture was analysed by gel electrophoresis (Pharmacia Biotech GNA-200 submarine unit with Power Pac 300 power supply, Bio-Rad) using a 2% (w/v) agarose gel and 1× Tris-acetate-EDTA (TAE) buffer (40 mM Tris-acetate, 1 mM EDTA, 50 mM NaCl).

Cytotoxicity test (MTT (3-(4,5-dimethylthiazol-2-yl)-2,5-tetrazolium bromide) assay). Cells were seeded in a 96-well flat-bottomed microplate at 20000 cells/well in 150 μL of growth medium solution (10% fetal calf serum (FCS, Gibco), 1% Sigma A-7292 Antibiotic and Antimycotic Solution in minimal essential medium (MEM-Eagle, Sigma)). Complexes **1**–**9** and cisplatin (positive control) were dissolved in DMSO (dimethyl sulfoxide) and mixed with the growth medium (final concentration ≤ 4% DMSO). Serial dilution of each complex was added to each well. The microplate was incubated at 37 °C, 5% CO_2, 95% air in a humidified incubator for 48 h. After incubation, 10 μL MTT reagent (5 mg/mL) was added to each well. The microplate was re-incubated at 37 °C in 5% CO_2 for 4 h. Solubilization solution (10% SDS in 0.01 M HCl) (100 μL) was added to each well. The microplate was left in an incubator for 24 h. Absorbances at 550 nm were measured by a microplate reader. The IC_{50} values of **1**–**9** (concentration required to reduce the absorbance by 50% compared to the controls) were determined by the dose-dependence of surviving cells after exposure to the metal complex for 48 h.

Flow cytometric analysis. The sheath fluid was an isotonic solution (Isoflow Coulter 8547008, Coulter Corporation). An excitation wavelength of 488 nm at 15 mW was used. About 10,000 cells were analysed in each sample. Cancer cells (NCI-H460 cell line) were cultured at a concentration of approximately 2×10^5 cells/mL. Complex **1** (0.1 μM) was added to the cultures. Staurosporin Streptomyces was used as positive control. After treatment, the cultures were incubated in 5% CO_2 at

37 °C. Cells were collected at 8 h interval. The genomic DNA was extracted according to the literature method,[1] and analysed by Annexin V plus PI staining.

cDNA microarray analysis. 3×10^7 cells were seeded in a 140 mm cell culture plate. Complex **1** (0.1 μM) was added to the cultures. Untreated cells were used as control. After treatment, the cultures were incubated in 5% CO_2 at 37 °C. Cells were collected at 8 h interval. TRIZOL reagent (Invitrogen, Gaithersburg, MD) was used to extract total RNA from the cultures according to the manufacturer's protocol.[8] Total RNA from control or treated cells were reverse-transcripted to cDNA in the presence of SuperScript II reverse transcriptase. During the reaction, two distinct fluorescent dyes, Cy3-dUTP and Cy5-dUTP (Amersham Pharmacia Biotech), were incorporated into the cDNA of the control and treated samples, respectively. The Cy3 and Cy5 labelled cDNA were combined and purified using Microcon 30 column (Microcon, MA) to final volume as 9 μL. The cDNA sample was mixed with a hybridization solution containing 1 μL of each of the following reagents: poly (dA) (8 mg/L), human Cot-1 DNA (4 mg/L), yeast tRNA (10 mg/L) and 3 μL of 20× SSC as well as 0.2 μL of 10% SDS. The mixture was then denatured at 100 ^{o}C for 2 min and applied to a microarray slide. Hybridization was performed at 65 ^{o}C for 16 h. Microarray images from two-color fluorescence hybridization were scanned with a confocal laser scanner (ScanArray 4000, GSI Lumonics, MA). The microarray results were analysed by using ScanAlyze (Michael Eisen, Standford University). Fluorescent images were gridded to locate the spot corresponding to each gene. Fluorescence and background intensities for both Cy3 and Cy5 wavelengths were extracted for data normalization and analysis. The raw data were filtered according to the following criteria: spots with small diameters (< 120 microns), low signal intensity (< 300 fluorescence intensity units), and low signal to noise ratio (< 1.5) were discarded. To ensure the reproducibility of the microarray results, the experiment was repeated with newly extracted total RNA samples. Fluorescence ratios (Cy5/Cy3) were used to determine the relative level of gene expression. Genes showed a greater than 2-fold induction or repression (Cy5/Cy3 ratios above 2 or below 0.5) were selected for further analysis.

Preparation of 4-ethynylphenoxy 2,3,4,6-tetra-*O*-acetyl-β-D-glucopyranoside (HL3)

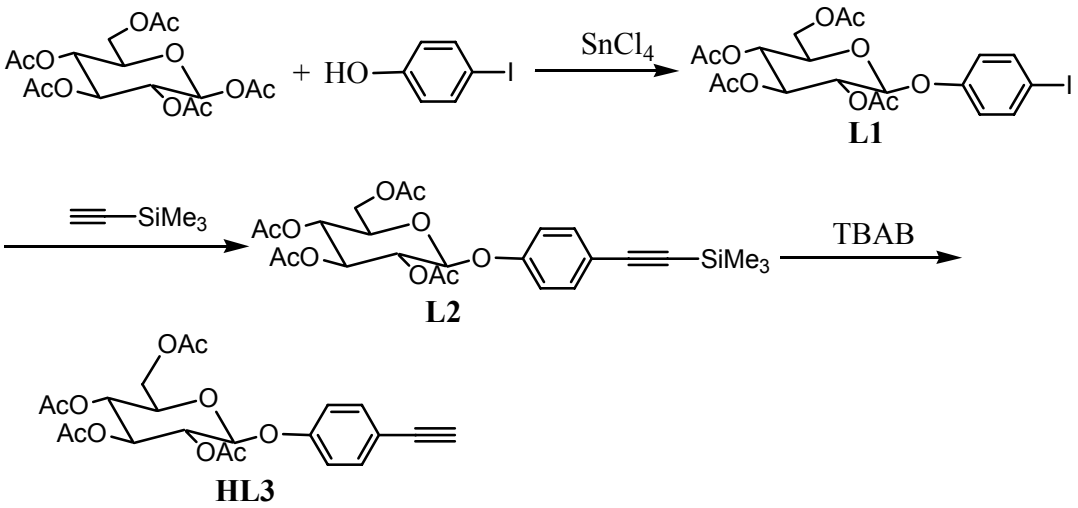

(a) 4-Iodophenyl 2,3,4,6-tetra-*O*-acetyl-β-D-glucopyranoside (L1). To a solution of β-D-glucopyranoside pentaacetate[3] (2 g, 5.13 mmol) and 4-iodophenol (1.58 g, 7.18 mmol) in dry

dichloromethane (10 mL) was added $SnCl_4$ (1.8 mL, 15.4 mmol). The reaction was stirred at room temperature. After completion of the reaction (monitored by TLC, petroleum/ethyl acetate = 2:1), the mixture was neutralised with aqueous $NaHCO_3$ and diluted with dichloromethane (20 mL). The solution was filtered through Celite and the filtered cake was washed with dichloromethane (10 mL). The organic phase was washed with brine, dried over Na_2SO_4, and evaporated. Flash column chromatography of the residue (hexane/ethyl acetate = 2:1) afforded a white solid, which was recrystallised from ethanol to give **L1** (1.20 g, 43%): Mp 182–183 ºC, $[\alpha]_D$ = –8.0 (c = 0.4, $CHCl_3$). IR (cm^{-1}, KBr): 3027 (ν_{ArH}), 2962 (ν_{C-H}), 1747 ($\nu_{C=O}$). ^1H NMR (400 MHz, $CDCl_3$): δ 2.03 (s, 3H), 2.05 (s, 3H), 2.06 (s, 3H), 2.08 (s, 3H) ($OCOCH_3$), 3.82–3.87 (m, 1H, H-5), 4.16 (dd, 1H, $J_{6a,5}$ = 2.4 Hz, $J_{6a,6b}$ = 12.0 Hz, H-6a), 4.27 (dd, 1H, $J_{6b,5}$ = 5.2 Hz, $J_{6b,6a}$ = 12.0 Hz, H-6b), 5.04 (d, 1H, $J_{1,2}$ = 8.0 Hz, H-1), 5.16 (t, 1H, $J_{4,5} = J_{4,3}$ = 9.2 Hz, H-4), 5.27–5.29 (m, 2H, H-2, H-3), 6.77 (d, 2H, J = 7.2 Hz, ArH), 7.58 (d, 2H, J = 7.2 Hz, ArH). ^{13}C NMR (100 MHz, $CDCl_3$): δ 20.7–20.8 (CH_3), 62.1 (C-6), 68.4 (C-4), 71.3 (C-3), 72.3 (C-5), 72.8 (C-2), 99.1 (C-1), 86.3, 119.4, 138.6, 156.8 (Ar), 169.3, 169.5, 170.3, 170.6 (CO). HRMS: Calcd. for $C_{20}H_{24}IO_{10}$ (M^+ + 1): 551.0414, found: 551.0414. Anal. Calcd. for $C_{20}H_{23}IO_{10}$: C, 43.65; H, 4.21. Found: C, 43.47; H, 4.18.

(b) 4-[(Trimethylsilyl)ethynyl]phenoxy 2,3,4,6-tetra-*O*-acetyl-β-D-glucopyranoside (L2). **L1** (0.8 g, 1.45 mmol) was dissolved in dry THF followed by addition of palladium acetate (18 mg, 8.0×10^{-5} mol), copper(I) iodide (12 mg, 6.3×10^{-5} mol) and triphenylphosphine (30 mg, 1.1×10^{-3} mol). The resulting solution was degassed with N_2 for 30 min and (trimethylsilyl)acetylene (0.23 mL, 1.62 mmol) was added. The mixture was stirred overnight at room temperature and filtered. The filtrate was evaporated and the residue was purified by column chromatography (hexane/ethyl acetate = 4:1→2:1) to afford a white solid, which was recrystallised from ethanol to give **L2** (0.63 g, 88%): Mp 213–214 ºC. IR (cm^{-1}, KBr): 3061 (ν_{ArH}), 2961, 2899 (ν_{C-H}), 2158 ($\nu_{C\equiv C}$), 1746 ($\nu_{C=O}$). ^1H NMR (300 MHz, $CDCl_3$): δ 0.24 (s, 9H, $SiMe_3$), 2.04 (s, 3H), 2.05 (s, 3H), 2.06 (s, 3H), 2.08 (s, 3H) ($OCOCH_3$), 3.87 (ddd, 1H, $J_{5,6b}$ = 2.4 Hz, $J_{5,6a}$ = 5.4 Hz, $J_{5,4}$ = 9.3 Hz, H-5), 4.16 (dd, 1H, $J_{6a,5}$ = 2.4 Hz, $J_{6a,6b}$ = 12.8 Hz, H-6a), 4.28 (dd, 1H, $J_{6b,5}$ = 5.4 Hz, $J_{6b,6a}$ = 12.8 Hz, H-6b), 5.08 (d, 1H, $J_{1,2}$ = 7.5 Hz, H-1), 5.16 (t, 1H, $J_{4,3} = J_{4,5}$ = 9.3 Hz, H-4), 5.26–5.30 (m, 2H, H-2, H-3), 6.90 (d, 2H, J = 7.2 Hz, ArH), 7.41 (d, 2H, J = 7.0 Hz, ArH). ^{13}C NMR (100 MHz, $CDCl_3$): δ 20.7–20.8 (CH_3), 62.1 (C-6), 68.4 (C-4), 71.3 (C-3), 72.3 (C-5), 72.8 (C-2), 93.7 (C≡C-$SiMe_3$), 98.9 (C-1), 104.6 (C≡C-$SiMe_3$), 116.8, 118.4, 133.6, 156.9 (Ar), 169.4, 169.5, 170.3, 170.7 (CO). HRMS: Calcd. for $C_{25}H_{33}O_{10}Si$ (M^+ + 1): 521.1843, found: 521.1909. Anal. Calcd. for $C_{25}H_{32}O_{10}Si$: C, 57.68; H, 6.20. Found: C, 57.66; H, 6.21.

(c) 4-Ethynylphenoxy 2,3,4,6-tetra-*O*-acetyl-β-D-glucopyranoside (HL3). **L2** (0.5 g, 0.96 mmol) was dissolved in dry dichloromethane (10 mL) and degassed for 10 min. Tetrabutylammonium fluoride (1.15 mL, 1.15 mmol) was added. The mixture was stirred at room temperature. After completion of the reaction (monitored by TLC, hexane/ethyl acetate = 1:1), the mixture was washed with brine, dried over Na_2SO_4, and evaporated. Flash column chromatography (hexane:ethyl acetate = 2:1) of the residue afforded a pale yellow solid (0.29 g, 64%): Mp 203–205 ºC, $[\alpha]_D$ = –14.7 (c = 0.4, $CHCl_3$). IR (cm^{-1}, KBr): 3286 ($\nu_{C\equiv CH}$), 3061 (ν_{ArH}), 2945 (ν_{C-H}), 2108 ($\nu_{C\equiv C}$), 1752 ($\nu_{C=O}$). ^1H NMR (300 MHz, $CDCl_3$): δ 2.04 (s, 3H), 2.05 (s, 3H), 2.06 (s, 3H), 2.07 (s, 3H) ($OCOCH_3$), 3.03 (s, 1H, C≡CH), 3.84–3.90 (m, 1H, H-5), 4.17 (dd, 1H, $J_{6a,5}$ = 2.4 Hz, $J_{6a,6b}$ = 12.3 Hz, H-6a), 4.28 (dd, 1H, $J_{6b,5}$ = 5.4 Hz, $J_{6b,6a}$ = 12.3 Hz, H-6b), 5.10 (d, 1H, $J_{1,2}$ = 7.5 Hz, H-1), 5.16 (t, 1H, $J_{4,5} = J_{4,3}$ = 9.6 Hz, H-4), 5.27–5.34 (m, 2H, H-2 and H-3), 6.93 (d, 2H, J = 8.7 Hz, ArH), 7.43 (d, 2H, J = 8.7 Hz, ArH). ^{13}C NMR (100 MHz, $CDCl_3$): δ 20.7–20.8 (CH_3), 62.1 (C-6), 68.4 (C-4), 71.2 (C-3), 72.3 (C-5), 72.8 (C-2), 76.7 (C≡CH), 83.1 (C≡CH), 98.8 (C-1), 116.9, 117.2, 133.7, 157.1 (Ar), 169.4, 169.5, 170.3, 170.6 (CO). HRMS: Calcd. for $C_{22}H_{25}O_{10}$ (M^+ + 1): 449.1448, found: 449.1448. Anal. Calcd. for $C_{22}H_{24}O_{10}$: C, 58.93; H, 5.39. Found: C, 58.82; H, 5.42.

Preparation of 2-propynyl 3,4,6-triacetate-2-acetamido-2-deoxy-β-D-glucopyranoside (HL4).

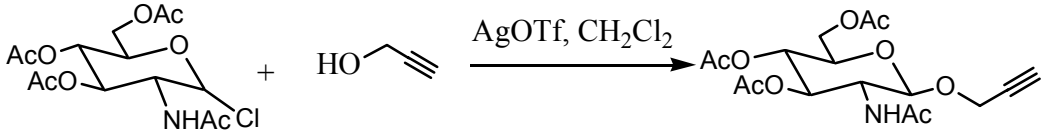

HL4

To a solution of 2,4,6-triacetate 2-acetamido-2-deoxy-α-D-glucopyranosyl chloride (2.0 g, 5.47 mmol) and propargyl alcohol (0.64 mL, 10.94 mmol) in dry dichloromethane (20 mL) at –10 ºC was added AgOTf (1.54 g, 6.0 mmol). After completion of the reaction (monitored by TLC, petroleum/ethyl acetate = 2:1), the mixture was neutralised with aqueous $NaHCO_3$, filtered, and the filtered cake was washed with dichloromethane. The resulting solution was separated and the water phase extracted with dichloromethane (2 × 5 mL). The combined organic solution was washed with brine and dried over Na_2SO_4. Removal of the solvent followed by purification with column chromatography (petroleum/ethyl acetate = 3:1) gave the product as a white solid (1.2 g, 57%): Mp 251–253 ºC, $[\alpha]_D$ = –49.0 (c = 0.4, $CHCl_3$). IR (cm^{-1}, KBr): 3285 ($\nu_{C\equiv CH}$), 3246 (ν_{NH}), 2129 ($\nu_{C\equiv C}$), 1747 ($\nu_{C=O}$). ^{1}H NMR (400 MHz, $CDCl_3$): δ 1.94 (s, 3H), 2.03 (s, 3H), 2.05 (s, 3H), 2.09 (s, 3H) ($OCOCH_3$), 2.50 (t, 1H, J = 2.5 Hz, C≡CH), 3.73–3.75 (m, 1H, H-5), 3.96 (dd, 1H, $J_{2,3}$ = 10.0 Hz, $J_{2,1}$ = 8.5 Hz, H-2), 4.15 (dd, 1H, $J_{6a,5}$ = 2.5 Hz, $J_{6a,6b}$ = 12.5 Hz, H-6a), 4.28 (dd, 1H, $J_{6b,5}$ = 5.0 Hz, $J_{6b,6a}$ = 12.5 Hz, H-6b), 4.38 (s, 2H, OCH_2), 4.87 (d, 1H, $J_{1,2}$ = 8.5 Hz, H-1), 5.09 (t, 1H, $J_{4,3}$ = $J_{4,5}$ = 10.0 Hz, H-4), 5.30 (t, 1H, $J_{3,2}$ = $J_{3,4}$ = 10.0 Hz, H-3), 5.86 (br s, 1H, NH). ^{13}C NMR (100 MHz, $CDCl_3$): δ 20.6, 20.7, 20.8, 23.3 (CH_3), 54.2 (C-2), 55.9 (CH_2O), 62.0 (C-6), 68.5 (C-4), 71.9 (C-5), 72.4 (C-3), 75.4 (C≡CH), 78.5 (C≡CH), 98.4 (C-1), 169.4, 170.4, 170.7, 170.9 (CO). HRMS: Calcd. for $C_{17}H_{24}NO_9$ (M^+ + 1): 386.1451, found: 386.1451. Anal. Calcd. for $C_{17}H_{23}NO_9$: C, 52.98; H, 6.02; N, 3.63. Found: C, 52.74; H, 6.04; N, 3.65.

Preparation of 1-(2-Prop-1-ynyl)-(2,3,4,6-tetra-*O*-acetyl-α-D-glucopyranosyl)-(1→4)-2,3,6-tri-*O*-acetyl-β-D-glucopyranoside (HL5).[9]

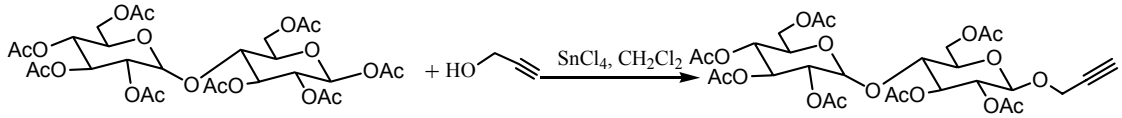

HL5

To a solution of β-D-maltose pentaacetate (12.0 g, 17.7 mmol) in dichloromethane (80 mL) was added $SnCl_4$ (2.1 mL, 17.7 mmol) with stirring at room temperature. After 10 min, propargyl alcohol (2 mL, 34.4 mmol) was added. On reaction completion (monitored by TLC, petroleum/ethyl acetate = 2:1), the reaction mixture was quenched with aqueous $NaHCO_3$, filtered, and washed with dichloromethane. The filtrate was separated and aqueous phase was extracted with dichloromethane (2 × 20 mL). The combined organic phase was dried over Na_2SO_4 and evaporated. Flash column chromatography (petroleum/ethyl acetate = 2:1) of the residue afforded **HL5** (6.5 g, 55%): Mp 104–105 ºC, $[\alpha]_D$ = +45.9 (c = 1.0, $CHCl_3$). IR (cm^{-1}, KBr): 3295 ($\nu_{C\equiv CH}$), 2122 ($\nu_{C\equiv C}$), 1751 ($\nu_{C=O}$). ^{1}H NMR (400 MHz, $CDCl_3$): δ 2.00–2.15 (seven singlets, 21H, $OCOCH_3$), 2.51 (t, 1H, J = 2.0 Hz, C≡CH), 3.71–3.74 (m, 1H, H-5'), 3.94–3.97 (m, 1H, H-5), 4.03–4.06 (m, 2H, H-6a', H-4), 4.23–4.26 (m, 2H, H-6b', H-6a), 4.35 (d, 2H, J = 2.0 Hz, OCH_2), 4.49 (dd, 1H, $J_{6b,5}$ = 2.8 Hz, $J_{6b,6a}$ = 12.0 Hz,

H-6b), 4.80 (d, 1H, J = 8.0 Hz, H-1), 4.84–4.87 (m, 2H, H-2, H-2'), 5.05 (t, 1H, $J_{4,3} = J_{4,5}$ = 10.0 Hz, H-4'), 5.28 (t, 1H, $J_{3,2} = J_{3,4}$ = 9.2 Hz, H-3), 5.36 (t, 1H, $J_{3',4'} = J_{3',2'}$ = 10.0 Hz, H-3'), 5.41 (d, 1H, $J_{1',2'}$ = 4.0 Hz, H-1'). HRMS: Calcd. for $C_{29}H_{39}O_{18}$ (M^+ + 1): 675.2136, found: 675.2136. Anal. Calcd. for $C_{29}H_{38}O_{18}$: C, 51.63; H, 5.68. Found: C, 51.41; H, 5.66.

Preparation of 4-ethynylphenoxy 2′,3′,4′,6′,2,3,6-hepta-*O*-acetyl-*β*-D-maltopyranoside (HL7).

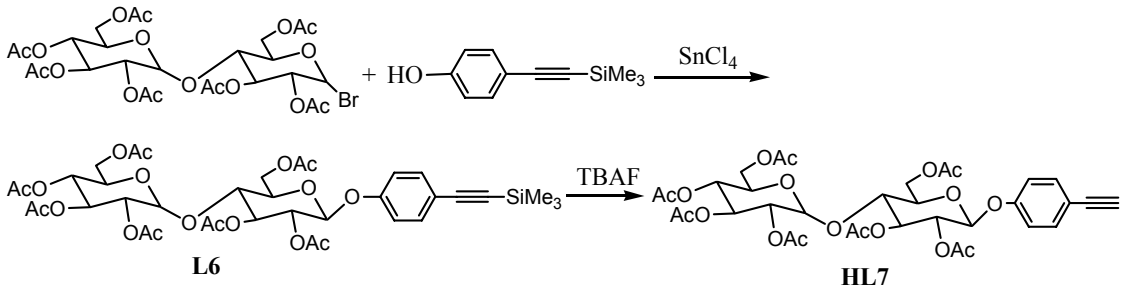

(a) [(Trimethylsilyl)ethynyl]phenoxy 2′,3′,4′,6′,2,3,6-hepta-*O*-acetyl-*β*-D-maltopyranoside (L6). To a solution of 2′,3′,4′,6′,2,3,6-hepta-*O*-acetyl-*α*-bromo-D-maltopyranose (3.0 g, 4.26 mmol) and 4-trimethylsilylethynylphenol[10] (0.96 g, 5.10 mmol) in dry dichloromethane (20 mL) and triethylamine (30 mL) was added Ag_2O (3.0 g, 12.9 mmol). The reaction mixture was stirred at room temperature. On reaction completion (TLC, hexane/ethyl acetate = 1:1), the mixture was filtered and the filtered cake was washed with dichloromethane (2 × 10 mL). The solvent was evaporated and the residue was purified by flash column chromatography (hexane/ethyl acetate = 2:1) to give a white solid (1.91 g, 55%): Mp 202–203 ºC, $[\alpha]_D$ = +47.6 (c = 1.0, $CHCl_3$). IR (cm^{-1}, KBr): 2965 (ν_{C-H}), 2156 ($\nu_{C\equiv C}$), 1751 ($\nu_{C=O}$). ^{1}H NMR (400 MHz, $CDCl_3$): δ 0.24 (s, 9H, $SiMe_3$), 2.00–2.10 (seven singlets, 21H, $OCOCH_3$), 3.87–3.91 (m, 1H, H-5), 3.96–3.98 (m, 1H, H-5'), 4.04–4.12 (m, 2H, H-6a', H-4), 4.23–4.28 (m, 2H, H-6b', H-6a), 4.47 (dd, 1H, $J_{6b,5}$ = 2.4 Hz, $J_{6b,6a}$ = 12.0 Hz, H-6b), 4.87 (dd, 1H, $J_{2',1'}$ = 4.0 Hz, $J_{2',3'}$ = 10.0 Hz, H-2'), 5.05 (t, 1H, $J_{4',3'} = J_{4',5'}$ = 10.0 Hz, H-4'), 5.09 (t, 1H, $J_{2,1} = J_{2,3}$ = 8.0Hz, H-2), 5.14 (d, 1H, $J_{1,2}$ = 8.0 Hz, H-1), 5.32 (t, 1H, $J_{3,2} = J_{3,4}$ = 8.0 Hz, H-3), 5.37 (t, 1H, $J_{3',2'} = J_{3',4'}$ = 10.0 Hz, H-3'), 5.43 (d, 1H, $J_{1',2'}$ = 4.0 Hz, H-1'), 6.90 (d, 2H, J = 8.4 Hz, ArH), 7.40 (d, 2H, J = 8.4 Hz, ArH). ^{13}C NMR (125 MHz, $CDCl_3$): δ 20.6–20.9 (CH_3), 61.6 (C-6'), 62.8 (C-6), 68.0 (C-4'), 68.6 (C-5'), 69.3 (C-3'), 70.0 (C-2'), 71.9 (C-2), 72.4 (C-5), 72.7 (C-4), 75.3 (C-3), 93.6 (C≡C-$SiMe_3$), 95.7 (C-1'), 98.1 (C-1), 104.4 (C≡C-$SiMe_3$), 116.7, 118.2, 133.5, 156.6 (Ar), 169.4, 169.6, 170.0, 170.2, 170.4, 170.5 (CO). HRMS: Calcd. for $C_{37}H_{49}O_{18}Si$ (M^+ + 1): 809.2688, found: 809.2688. Anal. Calcd. for $C_{37}H_{48}O_{18}Si$: C, 54.94; H, 5.98. Found: C, 54.84; H, 6.01.

(b) 4-Ethynylphenoxy 2′,3′,4′,6′,2,3,6-hepta-*O*-acetyl-*β*-D-maltopyranoside (HL7). L6 (1.0 g, 1.24 × 10^{-3} mol) was dissolved in dichloromethane (15 mL) and the solution was degassed for 10 min. Tetrabutylammonium fluoride (1.48 mL, 1.49 × 10^{-3} mol) was added and the mixture was stirred at room temperature. After completion of the reaction (monitored by TLC, hexane/ethyl acetate = 1:1), the mixture was washed with brine, dried over Na_2SO_4, and evaporated. The residue was purified by flash column chromatography (hexane/ethyl acetate = 2:1) to afford a white solid: (0.65 g, 71%). Mp 254–255 ºC, $[\alpha]_D$ = +46.3 (c = 1.0, $CHCl_3$). IR (cm^{-1}, KBr): 3283 ($\nu_{C\equiv CH}$), 3010 (ν_{ArH}), 2959 (ν_{C-H}), 2109 ($\nu_{C\equiv C}$), 1752 ($\nu_{C=O}$). ^{1}H NMR (400 MHz, $CDCl_3$): δ 2.01 (s, 3H), 2.03 (s, 3H), 2.04 (s, 3H), 2.05 (s, 3H), 2.08 (s, 3H), 2.09 (s, 3H), 2.10 (s, 3H) ($OCOCH_3$), 3.03 (s, 1H,

C≡CH), 3.87–3.91 (m, 1H, H-5), 3.96–3.99 (m, 1H, H-5'), 4.04–4.12 (m, 2H, H-6a', H-4), 4.23–4.28 (m, 2H, H-6b', H-6a), 4.47 (dd, 1H, $J_{6b,5}$ = 2.8 Hz, $J_{6b,6a}$ = 12.0 Hz, H-6b), 4.87 (dd, 1H, $J_{2',1'}$ = 4.0 Hz, $J_{2',3'}$ = 10.0 Hz, H-2'), 5.05 (t, 1H, $J_{4',3'} = J_{4',5'}$ = 10.0 Hz, H-4'), 5.09 (t, 1H, $J_{2,3} = J_{2,1}$ = 8.0 Hz, H-2), 5.14 (d, 1H, $J_{1,2}$ = 8.0 Hz, H-1), 5.32 (t, 1H, $J_{3,2} = J_{3,4}$ = 8.0 Hz, H-3), 5.37 (t, 1H, $J_{3',2'} = J_{3',4'}$ = 10.0 Hz, H-3'), 5.44 (d, 1H, $J_{1',2'}$ = 4.0 Hz, H-1'), 6.92 (d, 2H, J = 8.8 Hz, ArH), 7.43 (d, 2H, J = 8.8 Hz, ArH). ^{13}C NMR (125 MHz, $CDCl_3$): δ 20.6–20.9 (CH_3), 61.6 (C-6'), 62.8 (C-6), 68.0 (C-4'), 68.6 (C-5'), 69.3 (C-3'), 70.0 (C-2'), 71.9 (C-2), 72.4 (C-5), 72.7 (C-4), 75.2 (C-3), 76.7 (C≡CH), 83.0 (C≡CH), 95.7 (C-1'), 98.0 (C-1), 116.8, 117.0, 133.6, 156.8 (Ar), 169.4–170.5 (CO). HRMS: Calcd. for $C_{34}H_{41}O_{18}$ ($M^+ + 1$): 737.2293, found: 737.2292. Anal. Calcd. for $C_{34}H_{40}O_{18}$: C, 55.43; H, 5.47. Found: C, 55.36; H, 5.45.

Preparation of 4-ethynylphenoxy 2,3,4,6-tetra-*O*-acetyl-α-D-galactopyranoside (HL10).

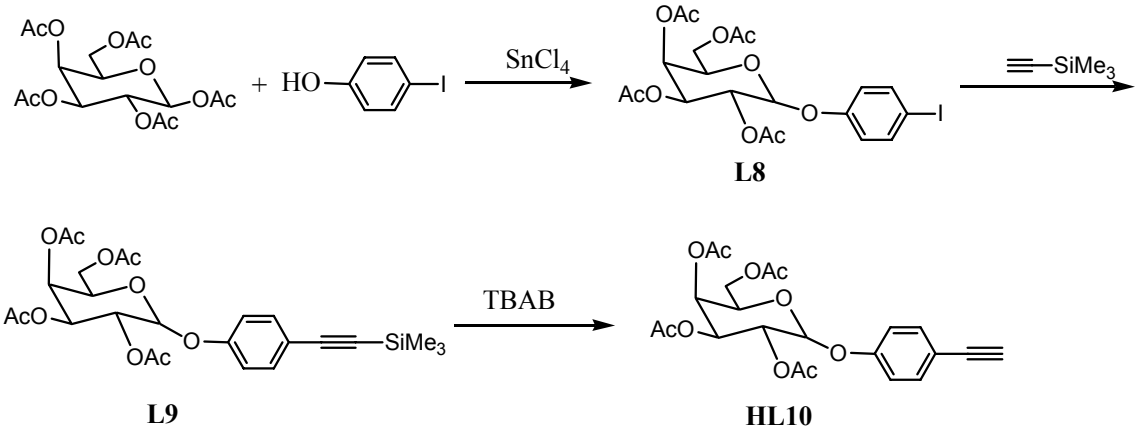

(a) 4-Iodophenyl 2,3,4,6-tetra-*O*-acetyl-α-D-galactopyranoside (L8). To a solution of β-D-galactopyranoside pentaacetate (4 g, 10.26 mmol) and 4-iodophenol (3.16 g, 14.4 mmol) in dry dichloromethane (20 mL) was added $SnCl_4$ (3.6 mL, 30.8 mmol). The reaction was stirred at room temperature. After completion of the reaction (monitored by TLC, petroleum/ethyl acetate = 2:1), the mixture was neutralised with aqueous $NaHCO_3$ and diluted with dichloromethane (20 mL). The solution was filtered through Celite and the filtered cake was washed with dichloromethane (20 mL). The organic phase was washed with brine, dried over Na_2SO_4, and evaporated. Flash column chromatography of the residue (hexane/ethyl acetate = 3:1→2:1) afforded the α-isomer of **L8**: (1.8 g, 32%). Mp 166–168 ºC, $[\alpha]_D$ = +179.2 (c = 1.0, $CHCl_3$). IR (cm^{-1}, KBr): 2966 (ν_{C-H}), 1749 ($\nu_{C=O}$). ^{1}H NMR (300 MHz, $CDCl_3$): δ 1.95 (s, 3H), 2.03 (s, 3H), 2.07 (s, 3H), 2.17 (s, 3H) ($OCOCH_3$), 4.03–4.14 (m, 2H, H-6), 4.29 (t, 1H, $J_{5,6a} = J_{5,6b}$ = 6.0 Hz, H-5), 5.27 (dd, $J_{3,2}$ = 10.0 Hz, $J_{3,4}$ = 3.6 Hz, H-3), 5.52–5.57 (m, 2H, H-2, H-4), 5.73 (d, 1H, $J_{1,2}$ = 3.6 Hz, H-1), 6.84 (d, 2H, J = 9.0 Hz, ArH), 7.6 (d, 2H, J = 9.0 Hz, ArH). ^{13}C NMR (125 MHz, $CDCl_3$): δ 20.6–20.7 (CH_3), 61.4 (C-6), 67.3 (C-5), 67.4 (C-2), 67.7 (C-3), 67.8 (C-4), 94.9 (C-1), 85.8, 119.0, 138.5, 156.1 (Ar), 170.0, 170.1, 170.3, 170.4 (CO). HRMS (EI): Calcd. for $C_{20}H_{23}IO_{10}$ (M^+): 550.0336, found: 550.0336. Anal. Calcd. for $C_{20}H_{23}IO_{10}$: C, 43.65; H, 4.21. Found: C, 43.50; H, 4.19.

(b) 4-[(Trimethylsilyl)ethynyl]phenoxy 2,3,4,6-tetra-*O*-acetyl-α-D-glucopyranoside (L9). **L8** (1.30 g, 2.35 mmol) was dissolved in dry THF followed by addition of palladium acetate (29 mg, 12.9×10^{-5} mol), copper(I) iodide (20 mg, 10.5×10^{-5} mol) and triphenylphosphine (48.7 mg, 1.8×10^{-3} mol). The resulting solution was degassed with N_2 for 30 min and (trimethylsilyl)acetylene

(0.36 mL, 2.53 mmol) was added. The mixture was stirred overnight at room temperature and filtered. The filtrate was evaporated and the residue was purified by chromatography (hexane/ethyl acetate = 2:1) to afford **L9**: (1.13 g, 92%). Mp 78–80 ºC, $[\alpha]_D$ = +202.8 (c = 1.0, $CHCl_3$). IR (cm^{-1}, KBr): 2961 (ν_{C-H}), 2157 ($\nu_{C\equiv C}$), 1751 ($\nu_{C=O}$). ^1H NMR (400 MHz, $CDCl_3$): δ 0.25 (s, 9H, $SiMe_3$), 1.95 (s, 3H), 2.03 (s, 3H), 2.07 (s, 3H), 2.17 (s, 3H) ($OCOCH_3$), 4.02–4.13 (m, 2H, H-6), 4.30 (br t, 1H, J = 6.8 Hz, H-5), 5.28 (dd, $J_{3,4}$ = 3.6 Hz, $J_{3,2}$ = 10.0 Hz, H-3), 5.51–5.57 (m, 2H, H-2, H-4), 5.77 (d, 1H, $J_{1,2}$ = 3.6 Hz, H-1), 6.98 (d, 2H, J = 8.8 Hz, ArH), 7.40 (d, 2H, ArH). ^{13}C NMR (125 MHz, $CDCl_3$): δ 20.6–20.7 (CH_3), 61.5 (C-6), 67.3 (C-5), 67.4 (C-2), 67.7 (C-3), 67.8 (C-4), 93.5 (C≡C-$SiMe_3$), 94.7 (C-1), 104.5 (C≡C-$SiMe_3$), 116.6, 117.8, 133.5, 156.2 (Ar), 170.0, 170.2, 170.3, 170.4 (CO). HRMS (EI): Calcd. for $C_{25}H_{32}O_{10}$ Si (M^+): 520.1765, found: 520.1764. Anal. Calcd. for $C_{25}H_{32}O_{10}Si$: C, 57.68; H, 6.20. Found: C, 57.64; H, 6.22.

(c) 4-Ethynylphenoxy 2,3,4,6-tetra-*O*-acetyl-α-D-galactopyranoside (HL10). L9 (1.10 g, 2.11 mmol) was dissolved in dry dichloromethane (20 mL) and degassed for 10 min. Tetrabutylammonium fluoride (2.60 mL, 2.60 mmol) was added. The mixture was stirred at room temperature. On reaction completion (monitored by TLC, hexane/ethyl acetate = 1:1), the mixture was washed with brine, dried over Na_2SO_4, and evaporated. Flash column chromatography (hexane:ethyl acetate, 2:1) of the residue afforded **HL10**: (0.64 g, 67%). Mp 179–181 ºC, $[\alpha]_D$ = +215.0 (c = 1.0, $CHCl_3$). IR (cm^{-1}, KBr): 3286 ($\nu_{C\equiv CH}$), 2958 (ν_{C-H}), 2106 ($\nu_{C\equiv C}$), 1750 ($\nu_{C=O}$). ^1H NMR (400 MHz, $CDCl_3$): δ 1.94 (s, 3H), 2.03 (s, 3H), 2.07 (s, 3H), 2.17 (s, 3H) ($OCOCH_3$), 3.03 (s, 1H, C≡CH), 4.03–4.14 (m, 2H, H-6), 4.30 (br t, 1H, J = 6.8 Hz, H-5), 5.29 (dd, 1H, $J_{3,4}$ = 3.6 Hz, $J_{3,2}$ = 10.0 Hz, H-3), 5.52–5.58 (m, 2H, H-2, H-4), 5.78 (d, 1H, $J_{1,2}$ = 3.6 Hz, H-1), 7.01 (d, 2H, J = 8.8 Hz, ArH), 7.43 (d, 2H, J = 8.8 Hz, ArH). ^{13}C NMR (100 MHz, $CDCl_3$): δ 20.7–20.8 (CH_3), 61.6 (C-6), 67.5 (C-5), 67.6 (C-2), 67.8 (C-3), 67.9 (C-4), 76.7 (C≡CH), 83.2 (C≡CH), 94.9 (C-1), 116.8, 116.9, 133.8, 156.6 (Ar), 170.1–170.5 (CO). HRMS (EI): Calcd. for $C_{22}H_{24}O_{10}$ (M^+): 448.1370, found: 448.1369. Anal. Calcd. for $C_{22}H_{24}O_{10}$: C, 58.93; H, 5.39. Found: C, 58.86; H, 5.41.

Preparation of platinum(II) complexes 1–5. To a solution of [Pt(^{t}Bu$_3$terpy)Cl](CF_3SO_3) (0.11 mmol) in CH_2Cl_2 (10 mL) were added **HL3**, **HL4**, **HL5**, **HL7** or **HL10** (0.17 mmol), CuI and anhydrous triethylamine (0.5 mL). The mixture was stirred at room temperature for 12 h under an argon atmosphere, and was then filtered. The solvent was evaporated to dryness. The product was isolated by column chromatography on silica gel using dichloromethane-methanol (10:1 v/v) as eluent.

[Pt(^{t}Bu$_3$terpy)(L3)](CF_3SO_3) (1). Yield: 94 mg (72%, orange solid). IR (cm^{-1}, KBr): 2122 ($\nu_{C\equiv C}$). ^1H NMR (400 MHz, $CDCl_3$): δ 1.49 (s, 18H), 1.58 (s, 9H), 2.05 (s, 3H), 2.06 (s, 3H), 2.08 (s, 3H), 2.10 (s, 3H), 3.87–3.92 (m, 1H), 4.19 (dd, 1H, J = 2.4 Hz, J = 12.0 Hz), 4.31 (dd, 1H, J = 5.2 Hz, J = 12.0 Hz), 5.10 (d, 1H, J = 8.0 Hz), 5.19 (t, 1H, J = 9.6 Hz), 5.26–5.34 (m, 2H), 6.95 (d, 2H, J = 8.0 Hz), 7.44 (d, 2H, J = 8.0 Hz), 7.61 (d, 2H, J = 6.0 Hz), 8.38 (s, 2H), 8.45 (s, 2H), 9.14 (d, 2H, J = 6.0 Hz). FAB-MS: m/z 1043 (M^+). Anal. Calcd. for $C_{50}H_{58}F_3N_3O_{13}PtS$: C, 50.33; H, 4.90; N, 3.52. Found: C, 50.30; H, 4.91; N, 3.61.

[Pt(^{t}Bu$_3$terpy)(L4)](CF_3SO_3) (2). Yield: 86 mg (69%, yellow solid). IR (cm^{-1}, KBr): 2130 ($\nu_{C\equiv C}$). ^1H NMR (300 MHz, $CDCl_3$): δ 1.48 (s, 18H), 1.56 (s, 9H), 1.94 (s, 3H), 2.03 (s, 3H), 2.04 (s, 3H), 2.16 (s, 3H), 3.82–3.94 (m, 2H), 4.12 (dd, 1H, J = 2.4 Hz, J = 12.0 Hz), 4.29 (dd, 1H, J = 4.5 Hz, J = 12.0 Hz), 4.68 (d, 1H, J = 15.0 Hz), 4.80 (d, 1H, J = 15.0 Hz), 5.09 (t, 1H, J = J = 9.6 Hz), 5.17 (d, 1H, J = 8.4 Hz), 5.45 (t, 1H, J = J = 9.6 Hz), 6.56 (d, 1H, J = 8.7 Hz), 7.74 (d, 2H, J = 6.0 Hz), 8.26 (s, 2H), 8.33 (s, 2H), 9.08 (d, 2H, J = 6.0 Hz). FAB-MS: m/z 980 (M^+). Anal. Calcd. for $C_{45}H_{57}F_3N_4O_{12}PtS$: C, 47.83; H, 5.08; N, 4.96. Found: C, 47.86; H, 5.08; N, 4.99.

[Pt(^{t}Bu$_3$terpy)(L5)](CF_3SO_3) (3). Yield: 103 mg (66%, yellow solid). IR (cm^{-1}, KBr): 2135 ($\nu_{C\equiv C}$). ^1H NMR (300 MHz, $CDCl_3$): δ 1.51 (s, 18H), 1.58 (s, 9H), 1.99 (s, 3H), 2.02 (s, 3H), 2.04 (s,

3H), 2.06 (s, 3H), 2.07 (s, 3H), 2.11 (s, 3H), 2.16 (s, 3H), 3.78–3.83 (m, 1H), 3.93–3.98 (m, 1H), 4.03–4.14 (m, 2H), 4.22–4.29 (m, 2H), 4.52 (dd, 1H, J = 3.0 Hz, J = 12.0 Hz), 4.74 (s, 2H), 4.87 (dd, 1H, J = 4.2 Hz, J = 10.0 Hz), 4.96–5.10 (m, 2H), 5.14 (d, 1H, J = 8.0 Hz), 5.32–5.39 (m, 2H), 5.47 (d, 1H, J = 4.0 Hz), 7.76 (d, 2H, J = 6.0 Hz), 8.38 (s, 2H), 8.45 (s, 2H), 9.07 (d, 2H, J = 6.0 Hz). FAB-MS: m/z 1271 (M^+). Anal. Calcd. for $C_{57}H_{72}F_3N_3O_{21}PtS$: C, 48.23; H, 5.11; N, 2.96. Found: C, 48.27; H, 5.12; N, 2.98.

[Pt(^{t}Bu$_3$terpy)(L7)](CF$_3$SO$_3$) (4). Yield: 111 mg (71%, orange solid). IR (cm^{-1}, KBr): 2116 ($\nu_{C\equiv C}$). ^{1}H NMR (300 MHz, $CDCl_3$): δ 1.50 (s, 18H), 1.60 (s, 9H), 2.02 (s, 3H), 2.04 (s, 3H), 2.05 (s, 3H), 2.06 (s, 3H), 2.07 (s, 3H), 2.11 (s, 3H), 2.12 (s, 3H), 3.88–3.92 (m, 1H), 3.97–4.01 (m, 1H), 4.05–4.16 (m, 2H), 4.23–4.32 (m, 2H), 4.52 (dd, 1H, J = 3.0 Hz, J = 12.0 Hz), 4.87 (dd, 1H, J = 4.2 Hz, J = 10.5 Hz), 5.07 (t, 1H, J = 10.0 Hz), 5.11–5.17 (m, 2H), 5.34 (t, 1H, J = 8.4 Hz), 5.39 (t, 1H, J = 9.0 Hz), 5.46 (d, 1H, J = 4.0 Hz), 6.94 (d, 2H, J = 9.0 Hz), 7.44 (d, 2H, J = 9.0 Hz), 7.81 (d, 2H, J = 6.0 Hz), 8.39 (s, 2H), 8.46 (s, 2H), 9.15 (d, 2H, J = 6.0 Hz). FAB-MS: m/z 1331 (M^+). Anal. Calcd. for $C_{62}H_{74}F_3N_3O_{21}PtS$: C, 50.27; H, 5.03; N, 2.84. Found: C, 50.28; H, 5.06; N, 2.92.

[Pt(^{t}Bu$_3$terpy)(L10)](CF$_3$SO$_3$) (5). Yield: 98 mg (75%, orange solid). IR (cm^{-1}, KBr): 2122 ($\nu_{C\equiv C}$). ^{1}H NMR (400 MHz, $CDCl_3$): δ 1.50 (s, 18H), 1.58 (s, 9H), 1.99 (s, 3H), 2.05 (s, 3H), 2.10 (s, 3H), 2.17 (s, 3H), 4.07–4.16 (m, 2H), 4.36 (br t, 1H, J = 6.8 Hz), 5.29 (dd, J = 12.0 Hz, J = 3.6 Hz), 5.54–5.61 (m, 2H), 5.80 (d, 1H, J = 3.6 Hz), 7.03 (d, 2H, J = 8.0 Hz), 7.47 (d, 2H, J = 8.0 Hz), 7.61 (d, 2H, J = 6.8 Hz), 8.37 (s, 2H), 8.44 (s, 2H), 9.14 (d, 2H, J = 6.8 Hz). FAB-MS: m/z 1043 (M^+). Anal. Calcd. for $C_{50}H_{58}F_3N_3O_{13}PtS$: C, 50.33; H, 4.90; N, 3.52. Found: C, 50.40; H, 4.86; N, 3.59.

Preparation of platinum(II) complexes 6 and 7. To a solution of [Pt(terpy)Cl](CF$_3$SO$_3$) (68 mg, 0.11 mmol) in CH_2Cl_2 (60 mL) were added **HL4** or **HL10** (0.17 mmol), CuI and anhydrous triethylamine (0.5 mL). The mixture was stirred at room temperature for 24 h under an argon atmosphere, and was then filtered. The volume of the filtrate was reduced. The product precipitated was collected by filtration, washed with water and diethyl ether, and recrystallised from methanol.

[Pt(terpy)(L4)](CF$_3$SO$_3$) (6). Yield: 59 mg (56%, brick-red solid). IR (cm^{-1}, KBr): 2136 ($\nu_{C\equiv C}$). ^{1}H NMR (400 MHz, CD_3SOCD_3): δ 1.93 (s, 3H), 1.95 (s, 3H), 1.97 (s, 3H), 2.01 (s, 3H), 3.76 (m, 1H), 3.92 (s, 1H), 4.22 (m, 1H), 4.40 (m, 1H), 4.51–4.60 (m, 2H), 4.93 (m, 2H), 5.24 (m, 1H), 7.86 (m, 1H), 8.09 (d, 2H, J = 7.0 Hz), 8.23–8.28 (m, 7H), 8.36 (s, 2H, J = 7.0 Hz). FAB-MS: m/z 812 (M^+). Anal. Calcd. for $C_{33}H_{33}F_3N_4O_{12}PtS$: C, 41.21; H, 3.46; N, 5.83; Found: C, 40.95; H, 3.60; N, 5.96.

[Pt(terpy)(L10)](CF$_3$SO$_3$) (7). Yield: 64 mg (57%, brick-red solid). IR (cm^{-1}, KBr): 2116 ($\nu_{C\equiv C}$). ^{1}H NMR (400 MHz, CD_3SOCD_3): δ 1.92 (s, 3H), 1.98 (s, 3H), 2.08 (s, 3H), 2.15 (s, 3H), 4.00–4.07 (m, 2H), 4.40–4.42 (m, 1H), 5.17–5.21 (m, 1H), 5.42–5.46 (m, 2H), 5.86 (br, 1H), 7.09 (d, 2H, J = 8.0 Hz), 7.42 (d, 2H, J = 8.0 Hz), 7.82–7.86 (m, 2H), 8.42–8.91 (m, 9H). FAB-MS: m/z 875 (M^+). Anal. Calcd. for $C_{38}H_{34}F_3N_3O_{13}PtS$: C, 44.53; H, 3.34; N, 4.10. Found: C, 44.83; H, 3.41, N, 4.29.

References

1 J. Sambrook, E. F. Fritsch, T. E. Maniatis, *Molecular Cloning, A Laboratory Manual, 2nd Ed.,* 1989, E.3 and E.10.
2 G. Felsenfeld, S. Z. Hirschman, *J. Mol. Biol.,* 1965, **13**, 407.
3 M. L. Wolfrom, A. Thompson, *Methods in Carbohydr. Chem*., 1963, 2, 211.
4 E. Fischer, G. Zemplen, *Ber*., 1910, **43**, 2534.
5 (a) H. K. Yip, L. K. Cheng, K. K. Cheung, C.-M. Che, *J. Chem. Soc., Dalton Trans*., 1993, 2933; (b) S.-W. Lai, M. C. W. Chan, K.-K. Cheung, C.-M. Che, *Inorg. Chem.,* 1999, **38**, 4262.

6 S. J. Busch, R. L. Barnhart, G. A. Martin, M. A. Flanagan, R. L. Jackson, *J. Biol. Chem*., 1990, **265**, 22474.
7 C. V. Kumar, E. H. Asuncion, *J. Am. Chem. Soc.,* 1993, **115**, 8547.
8 P. Hegde, R. Qi, K. Abernathy, C. Gay, *Biotechniques,* 2000, **29**, 548.
9 G. B. Giovenzana, L. Lay, D. Monti, G. Palmisano, L. Panza, *Tetrahedron,* 1999, **53**, 14123.
10 Y. S. Shin, M. J. Han, S.-K. Hong, *Chem. Mater.,* 2000, **12**, 1076.

Fig. S1 UV/Vis spectra of **1–7** in CH_2Cl_2 at 298 K.

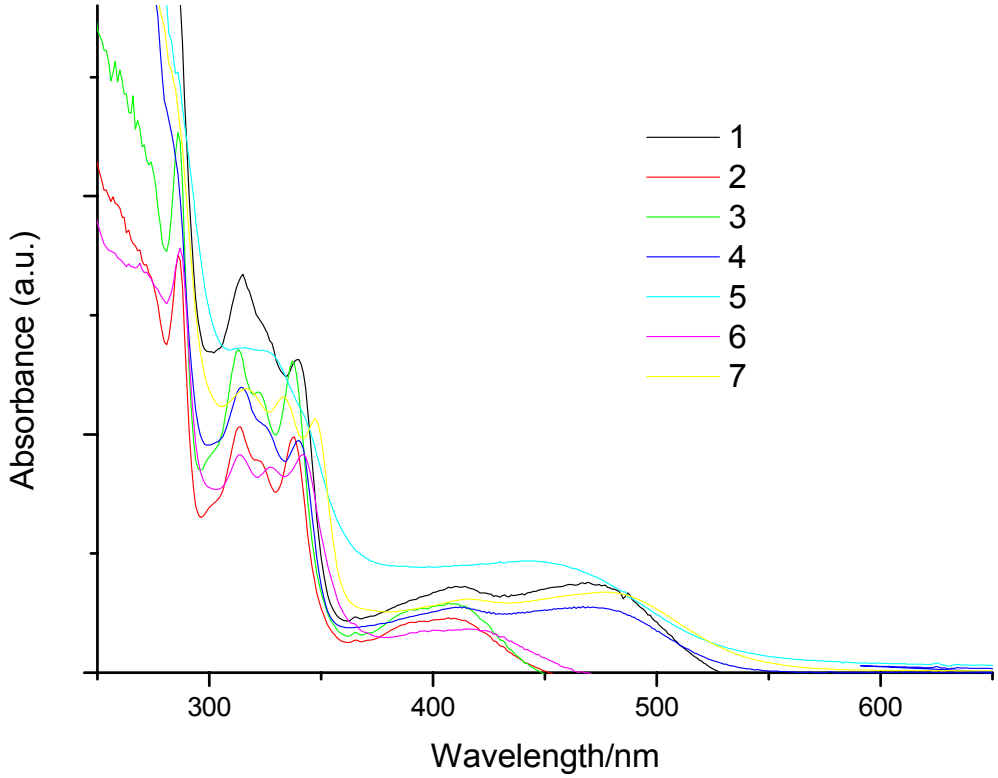

Fig. S2 UV/Vis spectra of **1–7** in H_2O at 298 K.

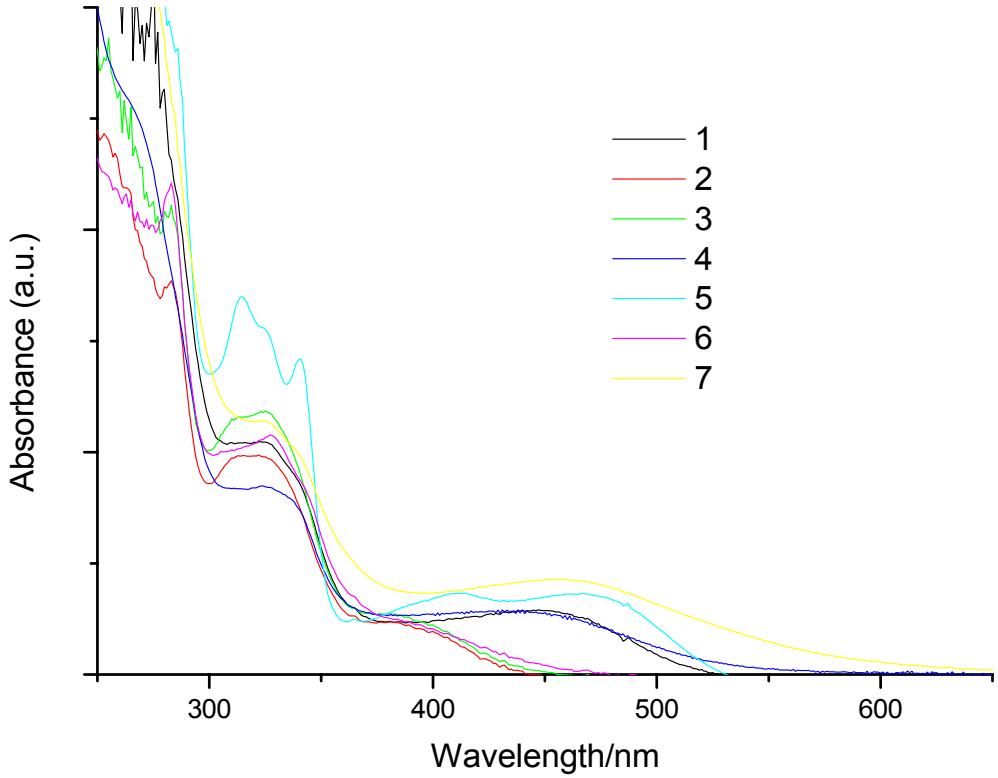

Fig. S3 Emission spectra of **1–7** in CH_2Cl_2 at 298 K.

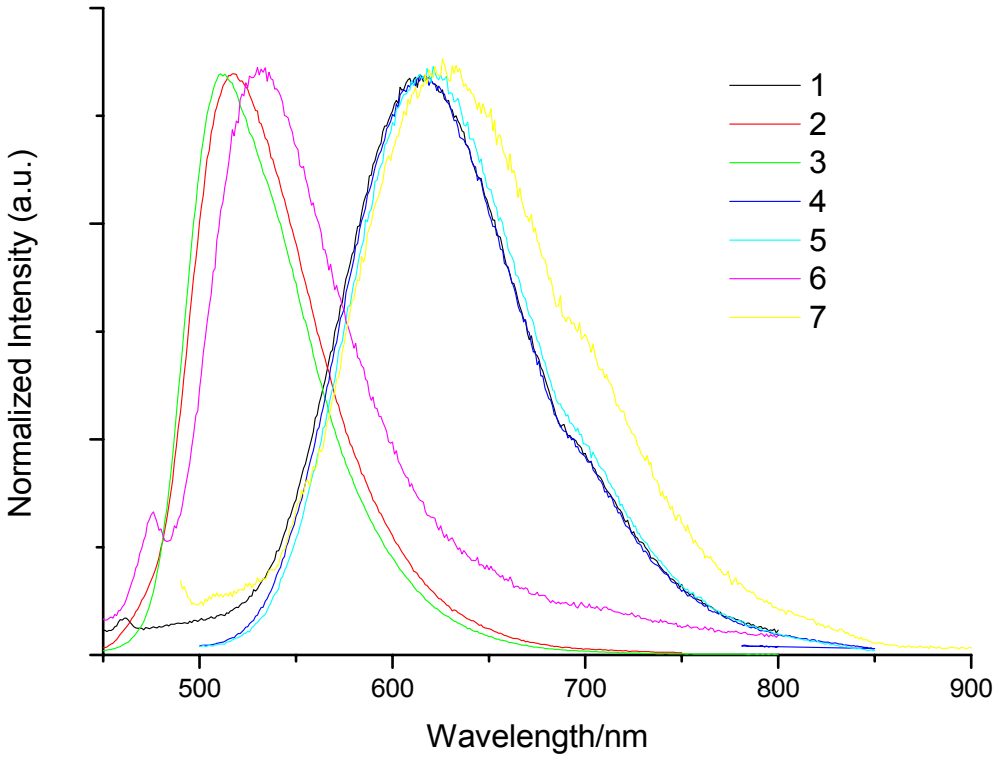

Fig. S4 Emission spectra of **1** in solid state and CH_2Cl_2 at 298 K.

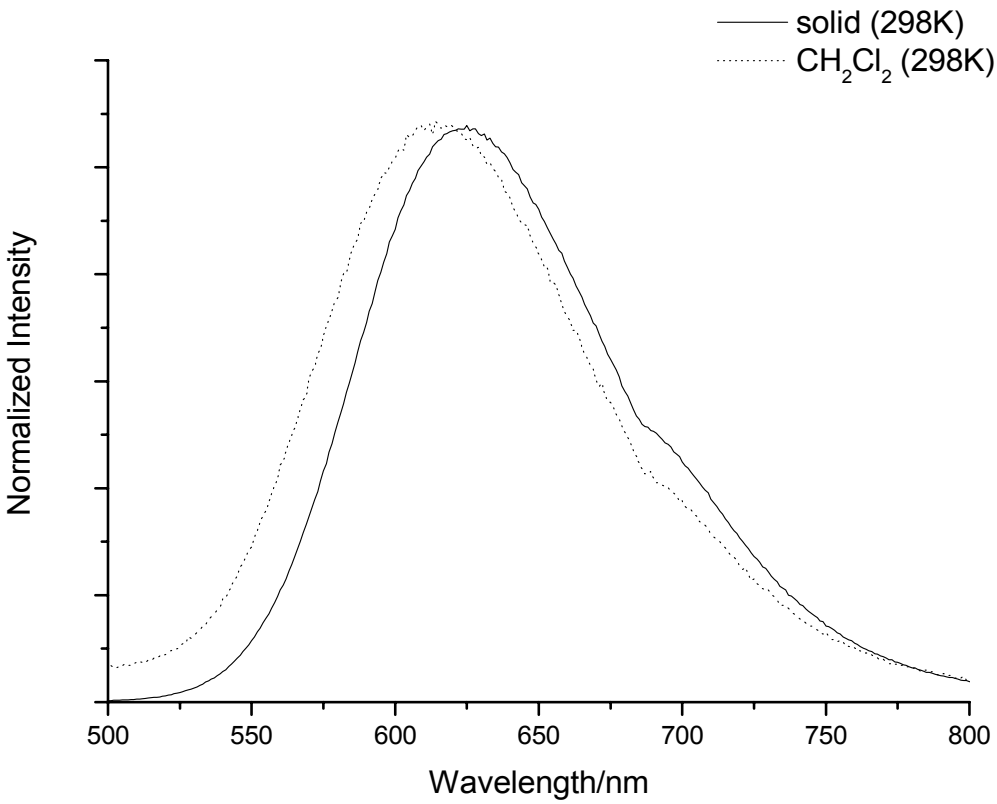

Fig. S5 Emission spectra of **1**, **4** and **5** in H_2O at 298 K.

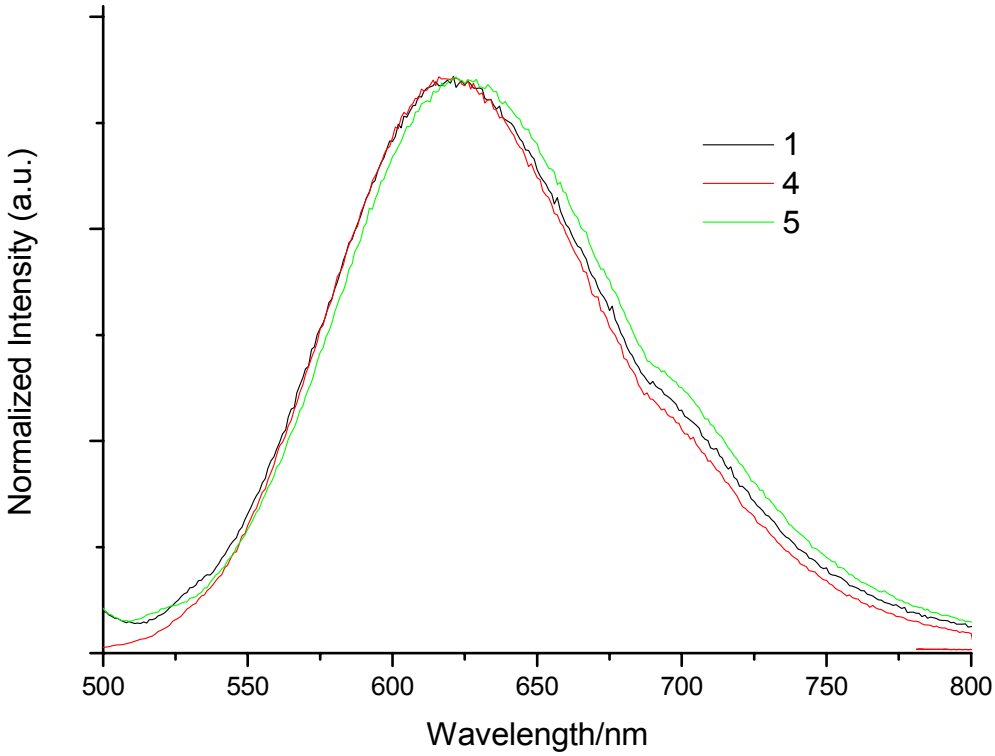

Fig. S6 Inhibition of restriction endonuclease ApaI cutting sites by various small molecules. Lane A is size marker. Lanes B and C are undigested and ApaI (1 unit/μL) digestion products of pDR2 DNA (10.7 kbp, 21 nM bp^{-1}), respectively.[a] Lanes D–F are the digestion products of pDR2 DNA in the presence of DNA interacting molecules: ethidium bromide (4 μM) (Lane D), Hoechst 33342 (200 μM) (Lane E), cisplatin (200 μM) (Lane F).[b] Lane G is the digestion products of pDR2 DNA in the presence of **1** at 4 μM (Lane G).[c]

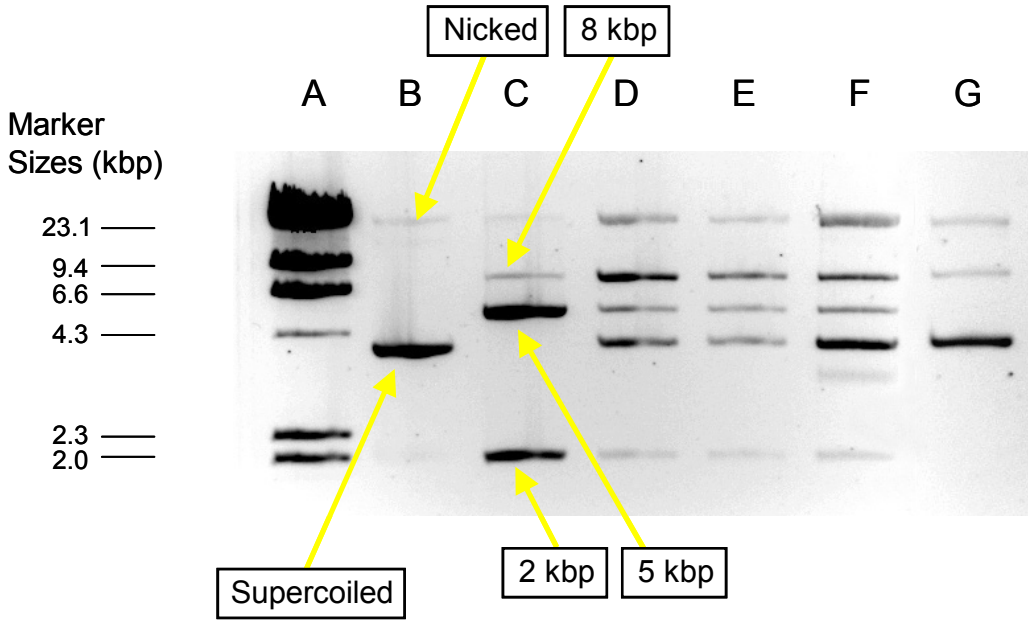

[a] Two bands corresponding to the supercoiled and nicked DNA were observed for the undigested DNA (Lane B). After ApaI digestion of pDR2, three bands corresponding to DNA fragments with 8, 5 and 2 kbp were obtained and resolved by agarose gel electrophorsis (Lane C).

[b] In the presence of the classical intercalator – ethidium bromide (4 μM), the minor groove binder – Hoechst 33342 (200 μM), or the intrastrand crosslinker – cisplatin (200 μM), DNA digestion was incomplete and bands attributed to the whole plasmid plus fragments were observed (Lanes D–F).

[c] Because complex **1** binds to DNA, treatment of pDR2 and ApaI with **1** at concentration 4 μM in 1× SuRE/Cut Buffer A inhibit the ApaI digestion and bands attributed to the whole plasmid plus fragments were observed (Lane G).

Fig. S7 UV/Vis spectra of **6** (50.0 μM) in Tris buffer solution with increasing ratio of [DNA]/[Pt] = 0–1.00 at 20.0 °C.

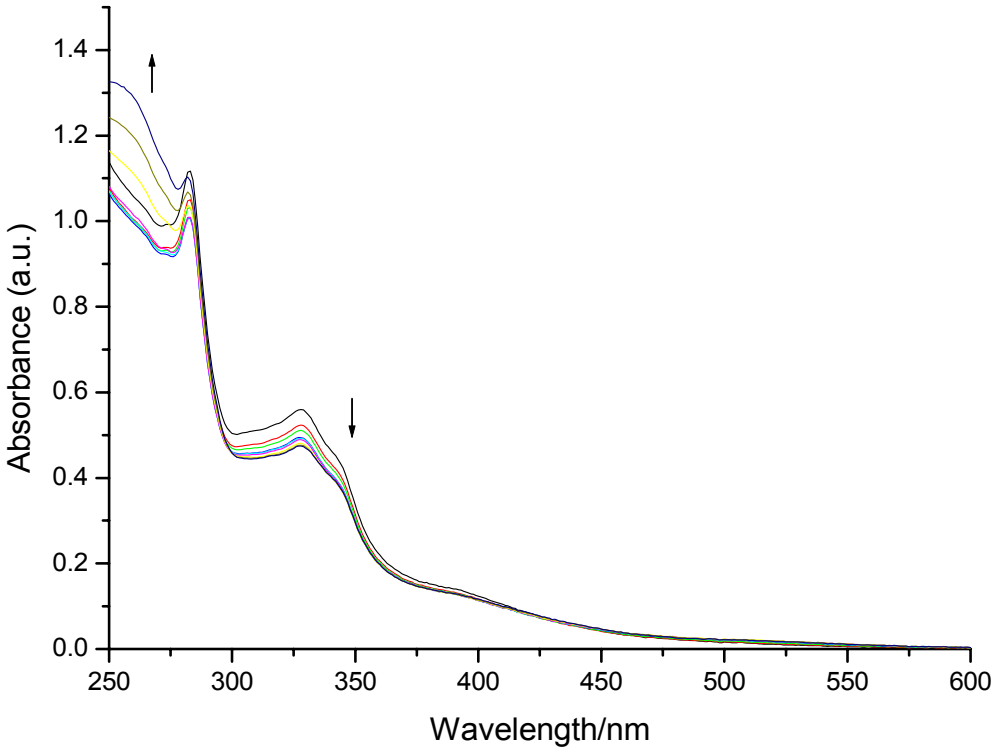

Fig. S8 UV/Vis spectra of **9** (50.0 μM) in Tris buffer solution with increasing ratio of [DNA]/[Pt] = 0–2.00 at 20.0 °C.

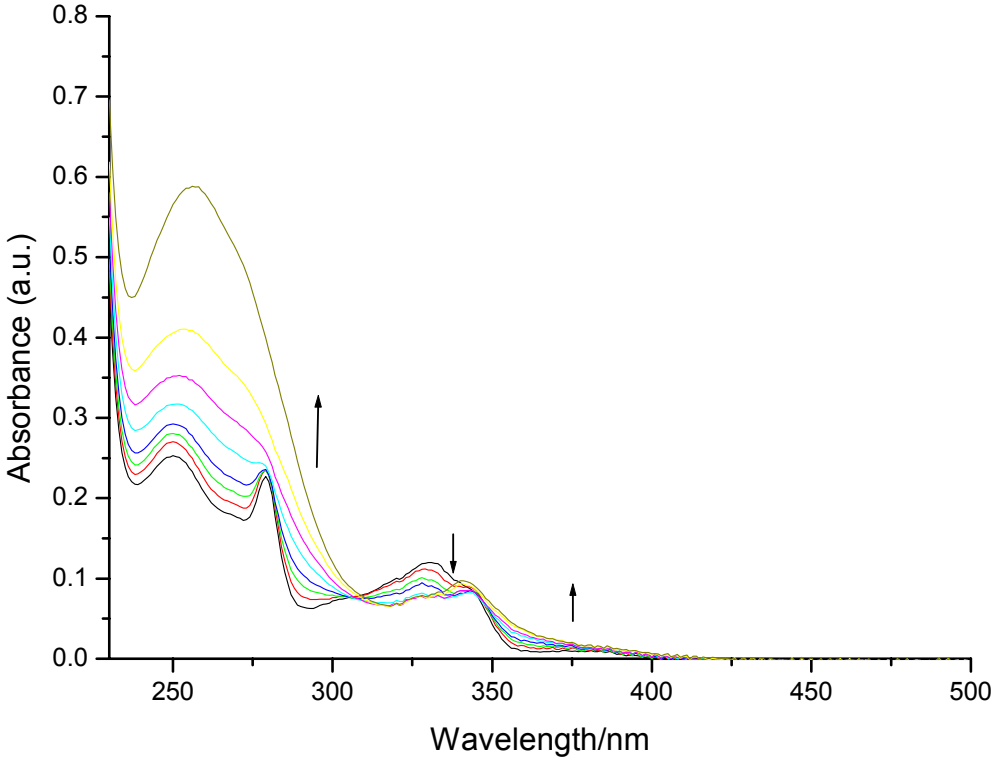

Fig. S9 Plot of $D/\Delta\varepsilon_{ap}$ vs. D. Absorbance was monitored at 325 nm.

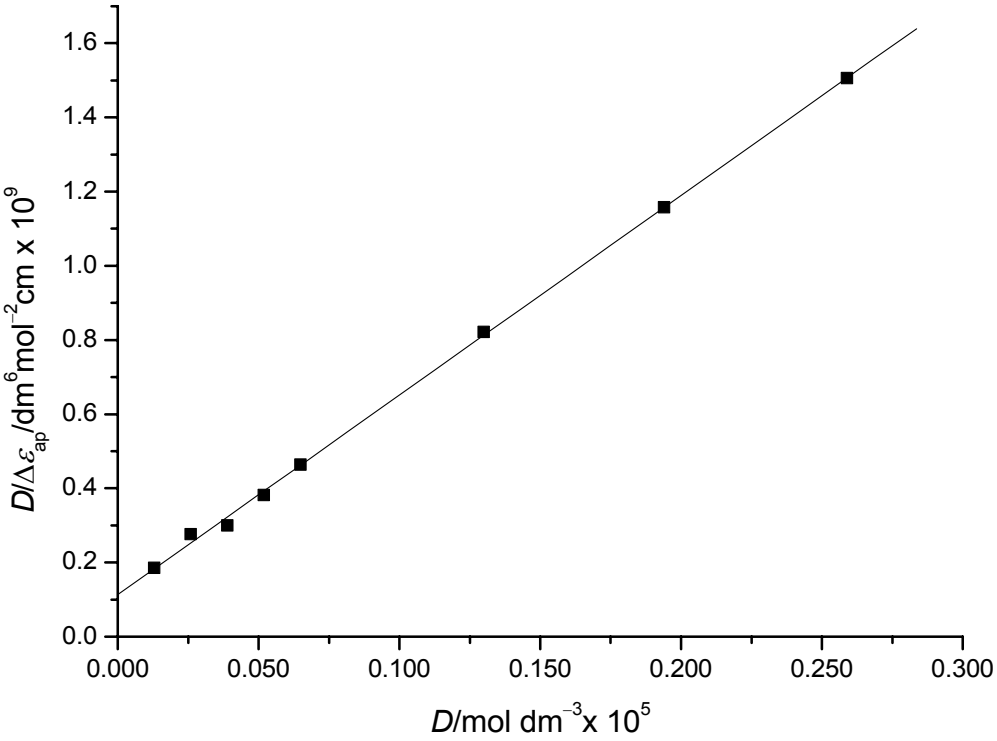

Fig. S10 Emission spectral traces of **1** (50 μM) in Tris buffer solution with increasing ratio of [DNA]/[**1**] = 0–5.4 at 20 ^{o}C. Inset: Plot of I/I_o vs [DNA]/[Pt] for the emission titration study of the **1**–DNA interaction.

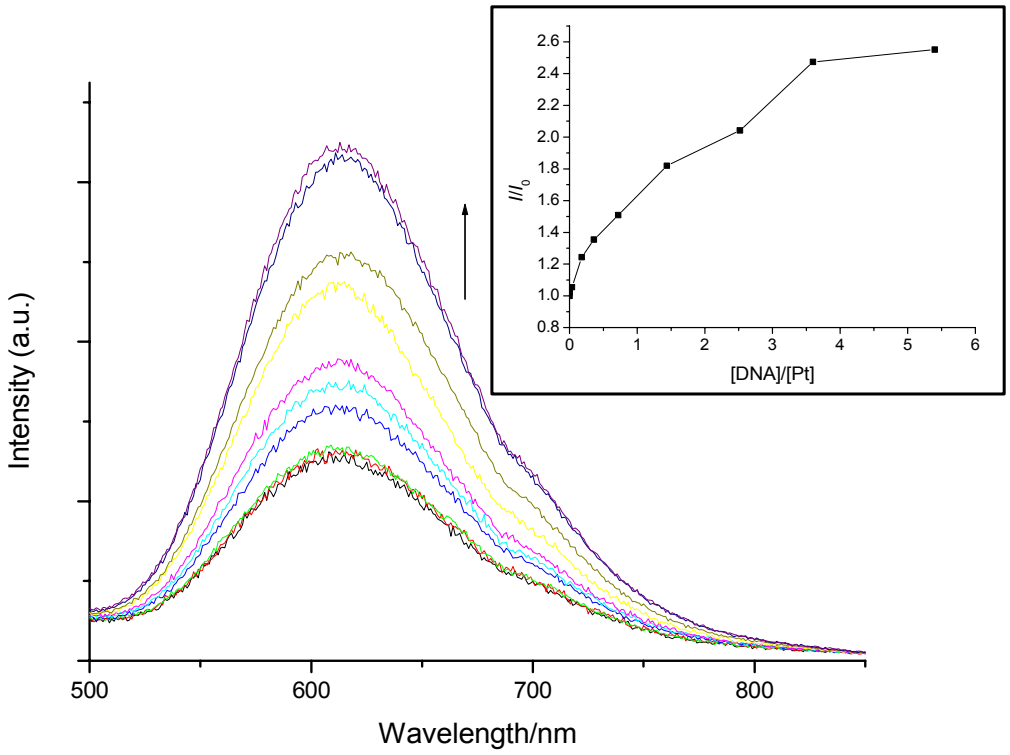

Fig. S11 Emission spectral traces of **7** (50.0 μM) in Tris buffer solution with increasing ratio of [DNA]/[Pt] = 0–5.1 at 20.0 °C. Inset: Plot of I/I_o vs [DNA]/[Pt] for the emission titration study of the **7**–DNA interaction.

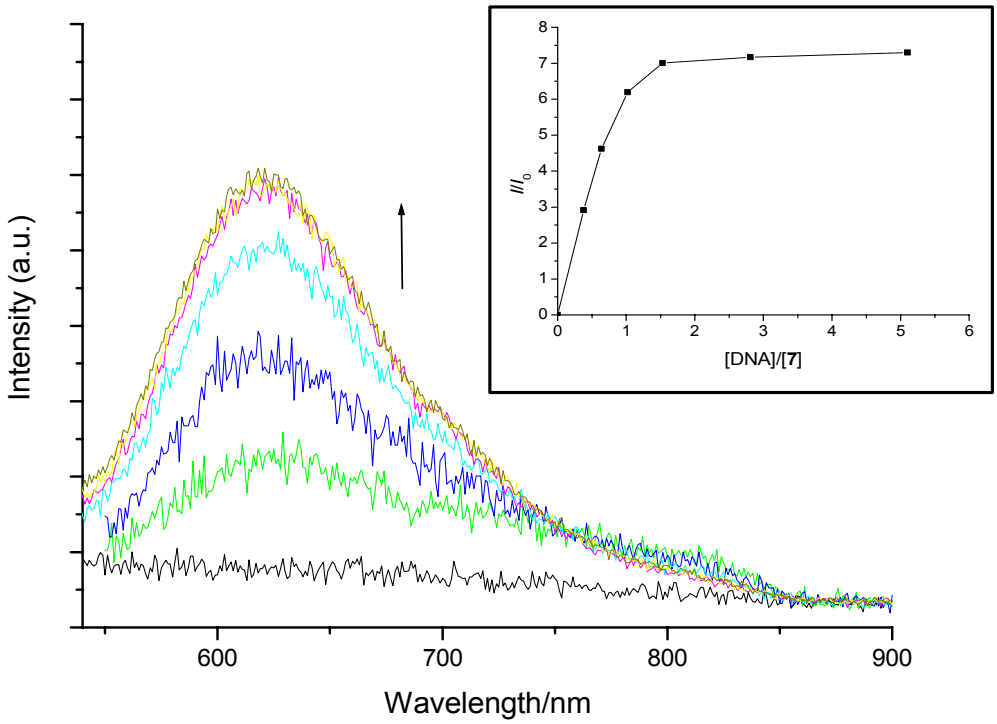

Fig. S12 FACS analysis of apoptotic NCI-H460 cells by Annexin-V-FLUOS and propidium iodide. (a) single parameter Annexin-V-Fluos (cultivation for 8 h in the presence of **1**), (b) dual parameter (cultivation for 8 h in the absence of **1**), and (c) dual parameter (cultivation for 8 h in the presence of **1**); cluster R1 = living cells, R2 = apoptotic cells, R3 = necrotic cells, and R4 = late apoptotic cells and necrotic cells.

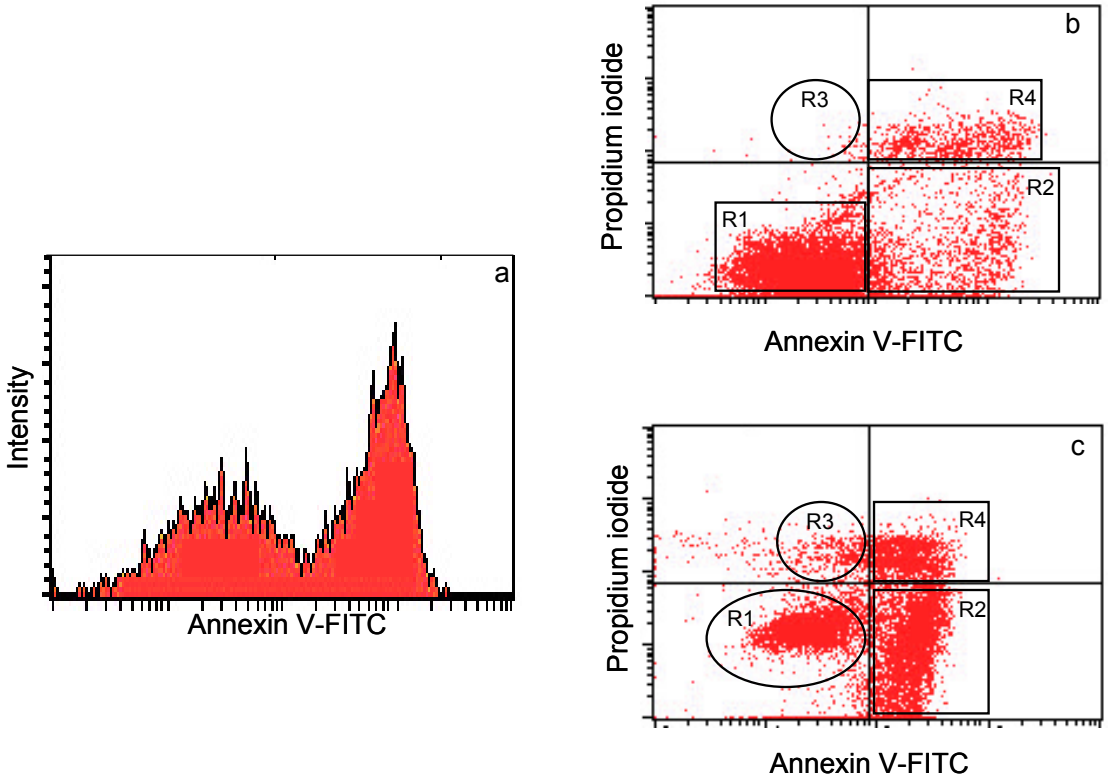

Fig. S13 Microarray image of a hybridization experiment with Cy3-labelled mRNA from treated by **1** in NCI-H460 cells and Cy5- labelled mRNA from untreated control NCI-H460 cells. The labelled mRNA pools were mixed and hybridised to a 10000 DNA microarray. Spots in green represent mRNAs in a relative higher abundance in the treated sample; spots in red represent mRNAs in a relative higher abundance in the control sample; yellow spots represent equal amounts of mRNA in both samples.

Human chip A

Cy3: complex **1**

Cy5: control

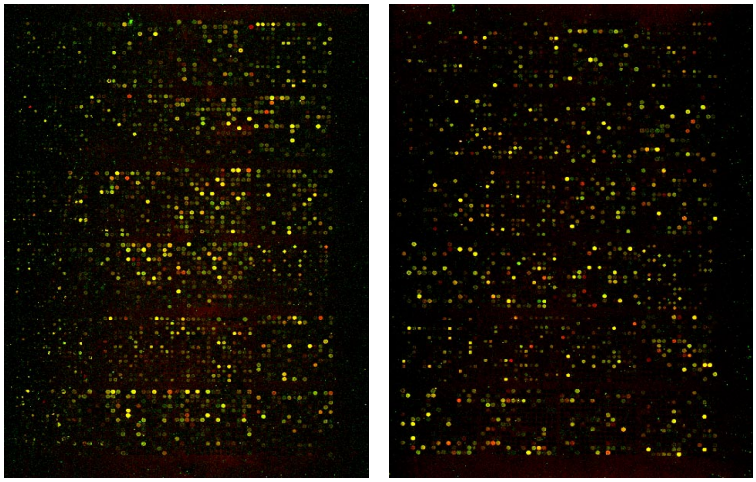

Human chip B

Cy3: complex **1**

Cy5: control

Table S1 Photophysical data for **1**–**7**

Complex	medium (T/K)	λ_{abs}/nm (ε_{max}/dm^3 mol^{-1} cm^{-1})	λ_{em}/nm (τ/μs)	ϕ_{em}
1	solid (298)		624 (0.17)	
	H_2O (298)	326 (104160), 341 (84040), 450 (28720)	619 (0.29)	3.7×10^{-2}
	CH_2Cl_2 (298)	314 (16650), 339 (13140), 412 (3710), 470 (3770)	615 ($\leq$ 0.2)[a]	4.4×10^{-2}
	CH_3CN (298)	310 (32500), 325 (31100), 338 (31500), 403 (8900), 440 (9300)	619 ($\leq$ 0.2)[a]	5.2×10^{-4}
	CH_3OH (298)	311 (37100), 325 (34300), 339 (33400), 404 (10300), 440 (9744)	624 (< 0.1)	4.8×10^{-4}
2	solid (298)		617 (0.30)	
	H_2O (298)	318 (9820), 382 (2310)	non-emissive	
	CH_2Cl_2 (298)	313 (10240), 322 (8880), 338 (9850), 409 (2300)	515 (0.23)	1.4×10^{-2}
3	solid (298)		613 (0.16)	
	H_2O (298)	312 (11760), 324 (118670), 380 (2730)	non-emissive	
	CH_2Cl_2 (298)	312 (13560), 323 (11690), 337 (13020), 411 (2870)	513 (0.45)	5.1×10^{-2}
4	solid (298)		638 (1.58)	
	H_2O (298)	324 (12270), 450 (3510)	621 (0.40)	1.2×10^{-2}
	CH_2Cl_2 (298)	316 (19940), 338 (16050), 408 (4970), 467 (5080)	617 (0.12)	2.4×10^{-3}
5	solid (298)		632 (0.26)	
	H_2O (298)	314 (17011), 324 (15590), 340 (14187), 411 (3694), 470 (3549)	623 (0.27)	1.4×10^{-2}
	CH_2Cl_2 (298)	326 (13578), 445 (4584)	619 (0.21)	2.4×10^{-2}
6	solid (298)		733 (< 0.1)	
	H_2O (298)	328 (10750), 342 (8510), 388 (2390)	non-emissive	
	CH_2Cl_2 (298)	313 (9150), 327 (8670), 342 (9150), 417 (1830)	532 (0.15)	1.6×10^{-1}
7	solid (298)		798 (< 0.1)	
	H_2O (298)	324 (14000), 455 (5200)	795 (< 0.1)	$< 1 \times 10^{-4}$
	CH_2Cl_2 (298)	316 (23800), 333 (23100), 348 (21200), 417 (6200), 476 (6800)	626 (< 0.1)	6.9×10^{-4}

[a] Not single exponential decay.

Table S2 Summary of DNA binding data for **1–9**

Complex	K at 20 °C/mol^{-1} dm^3
	Double-stranded DNA
1	n.d.[a]
2	8.3×10^4
3	9.2×10^4
4	1.3×10^6
5	n.d.[a]
6	4.8×10^5
7	3.7×10^5
8	6.9×10^5
9	3.9×10^5

[a] Not determined.

Table S3 Induction/repression of genes involved in diverse processes by **1** in NCI-H460 cells

Regulation	Gene Symbol	GenBank	Molecular Function	Biological Process	Cellular Component
Transcription					
+	DDIT3	BE410528	Transcription factor activity, Transcription corepressor activity	Cell cycle arrest, Cell growth and/or maintenance Regulation of transcription, DNA-dependent Response to DNA damage stimulus	Nucleus
+	ATF2	NM_001880	DNA binding RNA polymerase II transcription factor activity Transcription coactivator activity Zinc ion binding	Regulation of transcription, DNA-dependent	Nucleus
+	C20orf104	AI992137	Zinc ion binding DNA binding	Regulation of transcription, DNA-dependent	Nucleus
+	TCEA1	N41981	Transcription factor activity General RNA polymerase II transcription factor activity	Transcription RNA elongation Regulation of transcription from Pol II promoter	Nucleus
+	LRRFIP1	BG261015	Transcriptional repressor activity RNA polymerase II transcription factor activity Double-stranded RNA binding	Negative regulation of transcription Regulation of transcription from Pol II promoter	Cytoskeleton Nucleus
+	NCOA3	NM_006534	Thyroid hormone receptor binding Transcription coactivator activity Transferase activity Acyltransferase activity Histone acetyltransferase activity Signal transducer activity	Transcription Regulation of transcription, DNA-dependent Signal transduction Transcription	Nucleus
+	TGIF	AL549846	Transcription corepressor activity Transcription factor activity	Development Negative regulation of transcription from Pol II promoter Regulation of transcription,	Nucleus

				DNA-dependent	
+	ELL2	NM_012081	RNA polymerase II transcription factor activity	RNA elongation from Pol II promoter Regulation of transcription, DNA-dependent	Nucleus Transcription elongation factor complex
+	RXRG	NM_006917	Steroid binding Retinoid-X receptor activity Steroid hormone receptor activity Transcription factor activity	Regulation of transcription, DNA-dependent	Nucleus
+	T	NM_003181	Transcription factor activity	Mesoderm development Regulation of transcription, DNA-dependent Signal transduction Transcription from Pol II promoter Determination of anterior/posterior axis, embryo	Nucleus
–	ID1	AL117381	Regulation of transcription	Development	Nucleus
Protein biosynthesis					
+	GARS	NM_002047	Ligase activity ATP binding Glycine-tRNA ligase activity	Protein biosynthesis Glycyl-tRNA aminoacylation	Soluble fraction Cytoplasm
+	SPS2	BG674956	ATP binding Selenide, water dikinase activity Transferase activity	Selenocysteine biosynthesis	Cellular_component unknown
+	AARS	D32050	Alanine-tRNA ligase activity Ligase activity Nucleic acid binding TRNA binding ATP binding	Alanyl-tRNA aminoacylation Protein biosynthesis TRNA processing	Cytoplasm Soluble fraction
+	SIAT4A	NM_003033	Beta-galactoside alpha-2,3-sialyltransferase activity	Protein amino acid glycosylation	Integral to membrane Golgi apparatus

+	MARS	NM_004990	TRNA binding ATP binding Ligase activity Methionine-tRNA ligase activity	Methionyl-tRNA aminoacylation Protein biosynthesis	Soluble fraction Cytoplasm
–	TSFM	AU122778	Transcriptional elongation regulator activity Translation elongation factor activity	Protein biosynthesis Translational elongation	Mitochondrion
Oxidoreductase					
+	PYCR1	NM_006907	Pyrroline-5-carboxylate reductase activity Oxidoreductase activity	Proline biosynthesis	n.d.
+	SCD	AF097514	Iron ion binding Oxidoreductase activity Stearoyl-CoA 9-desaturase activity	Fatty acid biosynthesis	Endoplasmic reticulum Integral to membrane
+	MTHFD2	AL560341	Methylenetetrahydrofolate dehydrogenase (NAD+) activity Oxidoreductase activity Electron transporter activity Hydrolase activity Magnesium ion binding Methenyltetrahydrofolate cyclohydrolase activity	One-carbon compound metabolism Folic acid and derivative biosynthesis	Mitochondrion
Signaling					
+	ADAM15	BG766668	Metalloendopeptidase activity Protein binding Zinc ion binding SH3 domain binding Hydrolase activity	Proteolysis and peptidolysis Cell-matrix adhesion	Integral to membrane
+	PDE4D	U02882	3',5'-cyclic-nucleotide phosphodiesterase activity CAMP-specific phosphodiesterase activity Glutamyl-tRNA reductase activity Hydrolase activity	Signal transduction Cyclic nucleotide metabolism Porphyrin biosynthesis	Soluble fraction Insoluble fraction

+	DUSP3	AL555009	Hydrolase activity Protein tyrosine phosphatase activity Protein tyrosine/serine/threonine phosphatase activity	Protein amino acid dephosphorylation	n.d.
+	SQSTM1	BG164025	Protein kinase binding SH2 domain binding Ubiquitin binding Zinc ion binding	Endosome transport Intracellular signaling cascade Positive regulation of transcription from Pol II promoter Protein localization Regulation of I-kappaB kinase/NF-kappaB cascade Response to stress	Cytosol
+	STC2	AB012664	Hormone activity	Response to nutrients Cell surface receptor linked signal transduction Cell-cell signaling	Extracellular region
+	ARHGEF2	BG248725	Rac guanyl-nucleotide exchange factor activity Microtubule binding Rho GTPase binding Diacylglycerol binding Zinc ion binding	Cell surface receptor linked signal transduction Cellular morphogenesis Microtubule stabilization Regulation of Rho protein signal transduction Intracellular protein transport Intracellular signaling cascade Actin filament organization Regulation of cell proliferation	Microtubule
+	IL8	AV717082	Chemokine activity Protein binding Interleukin-8 receptor binding	Cell cycle arrest Cell motility Negative regulation of cell proliferation Cell-cell signaling Neutrophil activation Neutrophil chemotaxis Chemotaxis	Extracellular space Soluble fraction

				G-protein coupled receptor protein signaling pathway Regulation of cell adhesion Immune response Angiogenesis Regulation of retroviral genome replication Induction of positive chemotaxis Calcium-mediated signaling Intracellular signaling cascade	
+	AREG	AL546917	Cytokine activity Growth factor activity	Cell proliferation Cell-cell signaling	Extracellular space Integral to membrane
+	AREG	AL546917	Cytokine activity Growth factor activity	Cell proliferation Cell-cell signaling	Extracellular space Integral to membrane
+	SHOC2	AF068920	Molecular_function unknown	Ras protein signal transduction Fibroblast growth factor receptor signaling pathway	Cytoplasm
+	TJP1	NM_003257	Protein binding	Intercellular junction assembly	Membrane Membrane fraction Septate junction Tight junction
+	PKD1	AW963270	Sugar binding	Calcium-independent cell-matrix adhesion Homophilic cell adhesion Morphogenesis Neuropeptide signaling pathway	Integral to plasma membrane
+	SSI-3	AB006967	n.d.	Intracellular signaling cascade Regulation of cell growth	n.d.

+	SCYB5	BC008376	Chemokine activity	Immune response Inflammatory response Positive regulation of cell proliferation Signal transduction Cell-cell signaling Chemotaxis	Extracellular region
+	IL6	M54894	Interleukin-6 receptor binding Cytokine activity	Negative regulation of cell proliferation Positive regulation of cell proliferation Acute-phase response Cell surface receptor linked signal transduction Cell-cell signaling Humoral immune response	Extracellular space
+	DGKD	D63479	Protein binding Diacylglycerol binding Diacylglycerol kinase activity	Second-messenger-mediated signaling Diacylglycerol metabolism Epidermal growth factor receptor signaling pathway Cell growth Intracellular signaling cascade Immune response Development Protein homooligomerization Protein kinase C activation	Cytoplasm
+	FKBP8	BG326971	n.d.	Intracellular signaling cascade Protein folding	n.d.
+	APLP2	NM_001642	Serine-type endopeptidase inhibitor activity DNA binding Binding	G-protein coupled receptor protein signaling pathway	Integral to membrane Nucleus
+	OGT	NM_003605	Acetylglucosaminyltransferase activity Protein binding Transferase activity Transferase activity, transferring glycosyl groups	Response to nutrients Signal transduction O-linked glycosylation	Cytosol Nucleus

+	ZYX	NM_003461	Zinc ion binding Protein binding	Cell adhesion Cell-cell signaling Signal transduction	Integral to plasma membrane
+	NRGN	AW117600	Calmodulin binding	Signal transduction Neurogenesis	n.d.
–	MGST2	W73858	Transferase activity Enzyme activator activity Glutathione transferase activity	Antimicrobial humoral response (sensu Vertebrata) Cell-cell signaling Leukotriene biosynthesis Signal transduction	Integral to membrane Membrane fraction Microsome
–	YWHAH	NM_003405	Protein kinase C inhibitor activity Protein kinase binding Actin binding Insulin-like growth factor receptor binding Protein domain specific binding	Regulation of mitosis Regulation of neuron differentiation Cytoskeleton organization and biogenesis Regulation of signal transduction Regulation of synaptic plasticity Negative regulation of apoptosis Negative regulation of protein kinase activity	Cytoplasm
Cell cycle, proliferation, differentiation, growth					
+	PES1	NM_014303		Morphogenesis	Nucleus
+	ROD1	BG168693	mRNA processing	Morphogenesis	Nucleus RNA binding
+	FRAP1	NM_004958	Inositol or phosphatidylinositol kinase activity Transferase activity	DNA recombination DNA repair Regulation of cell cycle	Phosphoinositide 3-kinase complex
+	NOLC1	NM_004741	ATP binding GTP binding	Cell cycle Mitosis RRNA processing	Cytoplasm Nucleolus
+	BTG1	NM_001731		Cell growth and/or maintenance	
+	PPP2R4	AU125210	Phosphatase activator activity Protein phosphatase type 2A regulator activity Protein tyrosine phosphatase activator activity	Protein amino acid dephosphorylation	Soluble fraction

+	QSCN6	NM_002826	Electron transporter activity	Cell growth and/or maintenance Electron transport Negative regulation of cell proliferation Regulation of cell cycle Regulation of cell growth	Cellular_component unknown
–	STK15	NM_003600	Protein binding Protein serine/threonine kinase activity Transferase activity ATP binding	Cell cycle Mitosis Protein amino acid phosphorylation	Spindle Nucleus
–	CRIP1	BI222747	Zinc ion binding	Antimicrobial humoral response (sensu Vertebrata) Cell proliferation	Cytoplasm
–	S100A4	BG619887	Calcium ion binding	n.d.	n.d.
–	PCNA	NM_002592	DNA binding DNA polymerase processivity factor activity	Cell proliferation Regulation of DNA replication Regulation of cell cycle DNA repair DNA replication	Delta-DNA polymerase cofactor complex Nucleus
Apoptosis					
+	C20orf97	NM_021158	ATP binding Protein kinase binding Protein kinase inhibitor activity Transcription corepressor activity Protein binding Protein kinase activity	Activation of MAPK Apoptosis Negative regulation of protein kinase activity Regulation of transcription, DNA-dependent Protein amino acid phosphorylation	Nucleus
+	PEA15	BC002426	Protein binding Sugar porter activity	Regulation of apoptosis Transport Anti-apoptosis Negative regulation of glucose import	Microtubule associated complex
+	FN14	AI827127	Protein binding Receptor activity	Cell adhesion Cell motility Development Angiogenesis Apoptosis	Integral to membrane

+	PPM1F	NM_014634	Protein serine/threonine phosphatase activity Hydrolase activity Magnesium ion binding Manganese ion binding	Protein amino acid dephosphorylation Apoptosis	Protein serine/threonine phosphatase complex
Catabolism					
+	HMOX1	AU129800	Heme oxygenase (decyclizing) activity Oxidoreductase activity Signal transducer activity	Heme oxidation Positive regulation of I-kappaB kinase/NF-kappaB cascade	Membrane fraction Microsome Endoplasmic reticulum
Metabolism					
+	HDLBP	XM_042326	RNA binding Lipid transporter activity Nucleic acid binding	Lipid transport Cholesterol metabolism	Plasma membrane Nucleus
+	ASNS	NM_133436	Asparagine synthase (glutamine-hydrolyzing) activity Ligase activity	Glutamine metabolism Metabolism Asparagine biosynthesis	Soluble fraction
+	PYGB	BG575502	Phosphorylase activity Transferase activity, transferring glycosyl groups	Carbohydrate metabolism Glycogen catabolism	n.d.
+	GFPT1	NM_002056	Sugar binding Transferase activity Glutamine-fructose-6-phosphate transaminase (isomerizing) activity	Metabolism Carbohydrate biosynthesis Energy reserve metabolism Fructose 6-phosphate metabolism Glutamine metabolism	Cytoplasm
+	SHMT2	NM_005412	Transferase activity Glycine hydroxymethyltransferase activity	Glycine metabolism One-carbon compound metabolism L-serine metabolism	Mitochondrion
+	CPS1	BG761337	Ligase activity ATP binding Carbamoyl-phosphate synthase (ammonia) activity	Pyrimidine base biosynthesis Urea cycle Arginine biosynthesis	Mitochondrion
+	UGDH	NM_003359	Oxidoreductase activity	Glycosaminoglycan biosynthesis	n.d.

			UDP-glucose 6-dehydrogenase activity Electron transporter activity	UDP-glucose metabolism UDP-glucuronate biosynthesis Electron transport	
+	PSA	NM_058179	Phosphoserine transaminase activity Transferase activity	L-serine biosynthesis Metabolism Pyridoxine biosynthesis	n.d.
+	UP	BG492119	Transferase activity, transferring glycosyl groups□Uridine phosphorylase activity	Nucleoside metabolism Nucleotide catabolism	Cytoplasm
–	CYP7B1	NM_004820	Monooxygenase activity Oxysterol 7-alpha-hydroxylase activity	Bile acid biosynthesis Cholesterol metabolism Electron transport	Microsome Endoplasmic reticulum Membrane
–	NME4	AV704094	Kinase activity Nucleoside-diphosphate kinase activity Transferase activity ATP binding	Nucleoside metabolism CTP biosynthesis GTP biosynthesis UTP biosynthesis	Mitochondrion
–	GSTM2	NM_000848	Glutathione transferase activity Transferase activity	Metabolism	
Transport					
+	ATP6V0D1	NM_004691	Hydrogen-transporting ATPase activity, rotational mechanism Hydrogen-transporting ATP synthase activity, rotational mechanism Hydrolase activity	Proton transport ATP synthesis coupled proton transport	Proton-transporting two-sector ATPase complex
+	ATP2A2	NM_001681	Hydrolase activity ATP binding Hydrolase activity, acting on acid anhydrides, catalyzing transmembrane movement of substances Calcium ion binding Magnesium ion binding Calcium-transporting ATPase activity	Cation transport Cell adhesion Proton transport Epidermis development Transport Calcium ion transport Metabolism	Microsome Endoplasmic reticulum Integral to plasma membrane Membrane fraction
+	SLC1A4	NM_003038	Neutral amino acid transporter activity Sodium:dicarboxylate symporter activity Symporter activity	Dicarboxylic acid transport Neutral amino acid transport Transport	Integral to plasma membrane Membrane fraction
+	VAT1	NM_006373	DNA binding	Cell growth	Integral to

			NADPH:quinone reductase activity Alcohol dehydrogenase activity, zinc-dependent Oxidoreductase activity Zinc ion binding		membrane Nucleus Synaptic vesicle
+	VATI	BF725927	DNA binding NADPH:quinone reductase activity Alcohol dehydrogenase activity, zinc-dependent Oxidoreductase activity Zinc ion binding	Cell growth	Integral to membrane Nucleus Synaptic vesicle
+	ATP2B1	NM_001682	Calmodulin binding Hydrolase activity Hydrolase activity, acting on acid anhydrides, catalyzing transmembrane movement of substances ATP binding Magnesium ion binding Calcium ion binding Calcium-transporting ATPase activity	Cation transport Metabolism Calcium ion transport	Integral to plasma membrane
+	ATP6B2	BE899262	Hydrogen-transporting ATPase activity, rotational mechanism Hydrolase activity ATP binding Hydrogen-exporting ATPase activity, phosphorylative mechanism Hydrogen-transporting ATP synthase activity, rotational mechanism	ATP synthesis coupled proton transport Energy coupled proton transport, against electrochemical gradient	Proton-transporting two-sector ATPase complex Cytoplasm
+	SLC38A1	NM_030674	Sodium:amino acid symporter activity Neutral amino acid transporter activity Amino acid-polyamine transporter activity	Neutral amino acid transport Amino acid transport	Integral to membrane Membrane
+	ZNF263	NM_005741	Transcription factor activity Zinc ion binding	Regulation of transcription, DNA-dependent	Nucleus

+	PP15	BE409333	Protein transporter activity	Protein transport Protein-nucleus import	Nucleus
+	KPNB2	NM_153188	Nuclear localization sequence binding Protein transporter activity	Protein transport Protein-nucleus import, docking Protein-nucleus import, translocation	Cytoplasm Nuclear pore Nucleus
+	ALS2CR3	NM_015049	Intracellular transporter activity Receptor binding	Neurotransmitter transport	Cytoplasm Plasma membrane
+	SLC7A5	AB018009	Amino acid permease activity Neutral amino acid transporter activity	Amino acid metabolism Amino acid transport Transport	Integral to membrane Plasma membrane
+	KIAA0062	D31887	Metal ion transporter activity	Metal ion transport	Membrane
+	XPOT	NM_007235	TRNA binding	Transport	Nucleus
+	SLC3A2	NM_002394	Calcium:sodium antiporter activity Alpha-amylase activity	Carbohydrate metabolism Cell growth Amino acid transport Calcium ion transport	Integral to membrane
+	MB	NM_005368	Oxygen transporter activity Electron transporter activity	Oxygen transport Transport Muscle development	
Extracellular matrix, motility, cytoskeleton					
+	COL4A4	NM_000092	Extracellular matrix structural constituent	Phosphate transport Long-term strengthening of neuromuscular junction	Collagen Collagen type IV Cytoplasm
+	MYO1C	BE395925	Actin binding Calmodulin binding Motor activity ATP binding	Detection of sound	Unconventional myosin
+	ACTN1	AU118989	Actin binding Calcium ion binding Structural constituent of cytoskeleton	n.d.	Actin cytoskeleton

+	COL8A1	NM_001850	Protein binding Structural molecule activity	Phosphate transport Cell adhesion	Extracellular matrix (sensu Metazoa) Collagen type VIII Cytoplasm
+	SPTBN1	NM_003128	Structural constituent of cytoskeleton Actin binding Calmodulin binding	n.d.	Spectrin Cytoskeleton Membrane
–	ESTs	BC021909	GTP binding GTPase activity MHC class I protein binding Structural molecule activity	Microtubule polymerization Microtubule-based movement Natural killer cell mediated cytotoxicity	Tubulin
–	TUBB	BG762520	Unfolded protein binding GTP binding GTPase activity MHC class I protein binding Structural molecule activity	Microtubule polymerization Microtubule-based movement Natural killer cell mediated cytotoxicity	Tubulin
Other					
+	KIAA0731	AL133034	n.d.	n.d.	n.d.
+	KIAA0878	AU138104	GTPase activity Protein binding	Biological_process unknown	n.d.
+	ESTs	AU138357	Sodium:amino acid symporter activity Neutral amino acid transporter activity Amino acid-polyamine transporter activity	Neutral amino acid transport Amino acid transport	Integral to membrane Membrane
+	MGEA6	BF980666	3'-5'-exoribonuclease activity RNA binding Enzyme activator activity Protein binding	RNA processing	n.d.
+	KIAA0063	NM_014876	n.d.	n.d.	n.d.
+	NT5B	NM_012229	5'-nucleotidase activity Hydrolase activity	n.d.	Cytosol
+	MGC5139	NM_000017	Butyryl-CoA dehydrogenase	Electron transport Energy pathways	Mitochondrion

			activity Oxidoreductase activity	Fatty acid beta-oxidation Fatty acid metabolism	
+	KIAA0226	AI360844	n.d.	n.d.	n.d.
+	ESTs	BG434340	Transcriptional repressor activity Double-stranded DNA binding	Immune response Monocyte differentiation Regulation of transcription, DNA-dependent Response to virus Cell proliferation	Nucleus
+	unknown	unknown	n.d.	n.d.	n.d.
+	UBC	NM_021009			Nucleus
+	OAZIN	NM_148174	Catalytic activity Enzyme inhibitor activity	Polyamine biosynthesis Muscle development	n.d. n.d.
–	HSPC009	NM_014019	n.d.	n.d.	n.d.
–	MLP	NM_023009	Calmodulin binding	n.d.	n.d.
–	PCYT1B	AL521633	Transferase activity Choline-phosphate cytidylyltransferase activity	Phospholipid biosynthesis Phosphatidylcholine biosynthesis Biosynthesis	Endoplasmic reticulum
–	unknown	unknown	n.d.	n.d.	n.d.